

Washington University in St. Louis

Washington University Open Scholarship

All Theses and Dissertations (ETDs)

January 2010

Arsenic Removal From Drinking Water By Electrocoagulation

Wei Wan

Washington University in St. Louis

Follow this and additional works at: <https://openscholarship.wustl.edu/etd>

Recommended Citation

Wan, Wei, "Arsenic Removal From Drinking Water By Electrocoagulation" (2010). *All Theses and Dissertations (ETDs)*. 511.

<https://openscholarship.wustl.edu/etd/511>

This Thesis is brought to you for free and open access by Washington University Open Scholarship. It has been accepted for inclusion in All Theses and Dissertations (ETDs) by an authorized administrator of Washington University Open Scholarship. For more information, please contact digital@wumail.wustl.edu.

WASHINGTON UNIVERSITY IN ST. LOUIS
School of Engineering
Department of Energy, Environmental, and Chemical Engineering

Thesis Examination Committee:
Dr. Daniel E. Giammar, Chair
Dr. Young-Shin Jun
Dr. Palghat Ramachandran

A THESIS ON THE ARSENIC REMOVAL FROM DRINKING WATER BY
ELECTROCOAGULATION

by
Wei Wan

A thesis presented to the School of Engineering
of Washington University in partial fulfillment of the
requirements for the degree of
MASTER OF SCIENCE

May 2010
Saint Louis, Missouri

Abstract

A Thesis on the Arsenic Removal from Drinking Water by Electrocoagulation
by
Wei Wan
Master of Science in Energy, Environmental, and Chemical Engineering
Washington University in St. Louis, 2010
Research Advisor: Dr. Daniel E. Giammar

Exposure to arsenic through drinking water poses a threat to human health.

Electrocoagulation is an emerging water treatment technology that involves electrolytic oxidation of anode materials and *in-situ* generation of coagulant. Electrocoagulation is an alternative to using chemical coagulants for arsenic removal and thus is beneficial for communities with better access to electricity than to chemicals.

Batch electrocoagulation experiments were performed in the laboratory using iron electrodes. The experiments quantified the effects of pH, initial arsenic concentration and oxidization state, and concentrations of dissolved phosphate, silica and sulfate on the rate and extent of arsenic removal. The effect of water chemistry and treatment time were interpreted using adsorption modeling and a rate model for coagulant production and arsenic adsorption. The iron generated during electrocoagulation precipitated as lepidocrocite (γ -FeOOH), except when dissolved silica was present. Arsenic was removed by adsorption to the lepidocrocite. Arsenic removal was slower at higher pH. When solutions initially contained As(III), a portion of the As(III) was oxidized to As(V) during electrocoagulation. As(V) removal was faster than As(III) removal. The presence of 1 and 4 mg P/L of phosphate inhibited arsenic removal, while the presence of 5 and 20 mg SiO₂/L of silica or 10 and 50 mg SO₄²⁻/L of sulfate had no significant effect on

arsenic removal. The rate model simulated the overall arsenic removal by electrocoagulation well by using Faraday's law to predict coagulant production and a rate expression for As adsorption.

Equilibrium As(V) adsorption was investigated in batch experiments as a function of dissolved As(V) concentration, pH, and phosphate using lepidocrocite generated by electrocoagulation. A surface complexation model was then developed that successfully simulated equilibrium As(V) adsorption. As(V) adsorption onto the lepidocrocite generally decreased with increasing pH from 4 to 10. The presence of 1-4 mg P/L of phosphate inhibited As(V) adsorption. A maximum arsenic removal efficiency of over 99 % was achieved during both electrocoagulation and equilibrium adsorption experiments.

Acknowledgments

I would like to appreciate all those who have supported me as I pursued my Master degree at Washington University in St. Louis. Firstly, I would like to acknowledge the Department of Energy, Environmental, and Chemical Engineering at Washington University in St. Louis for providing me the opportunity to undertake my graduate study. I also thank the McDonnell Academy Global Energy and Environment Partnership of Washington University for financially supporting this project.

I appreciate my advisor Dr. Giammar very much for providing assistance as I worked on this project. I also thank all those who worked in the Aquatic Chemistry Lab, particularly Kate Nelson for providing analytical assistance, and Troy J. Pepping for providing experimental assistance. I would also like to thank Dr. Jun and Dr. Ramachandran for taking the time to review this thesis and attend my presentations. Thanks also go to Sanjeev Chaudhari from Indian Institute of Technology Bombay, India for his helpful suggestions to this project.

In the end, I would also like to thank my friends and family for providing consistent support to me.

Wei Wan

Washington University in St. Louis
May 2010

Contents

Abstract	ii
Acknowledgments	iv
List of Tables	vii
List of Figures	viii
Chapter 1	1
1.1 Background	1
1.2 Objectives.....	4
1.3 References	5
Chapter 2	7
2.1 Introduction	9
2.2 Materials and Methods.....	11
2.2.1 Laboratory-scale Electrocoagulation Experiments	11
2.2.2 Materials and Methods of the Field Study	13
2.2.3 Analysis Methods.....	15
2.3 Results and discussion.....	16
2.3.1 Production of Iron Oxide Coagulant.....	16
2.3.2 Effect of pH on As Removal.....	19
2.3.3 Effect of Oxidization State on As Removal.....	22
2.3.4 Effect of Initial As Concentrations on As Removal	24
2.3.5 Effect of Phosphate on As Removal	24
2.3.6 Effect of Silica on As Removal	26
2.3.7 Effect of Sulfate on As Removal	28
2.3.8 Results of the Field Study	29
2.4 Conclusions	31
2.5 Acknowledgments.....	31
2.6 References	32
Chapter 3	33
3.1 Introduction	36
3.2 Materials and Methods.....	37
3.2.1 Electrocoagulation Experiments	37
3.2.2 Equilibrium Adsorption Experiments	38
3.2.3 Sampling Methods	39

3.2.4	Analysis Methods.....	40
3.3	Results and Discussion.....	40
3.3.1	Production of Iron Oxide Coagulants by Electrocoagulation.....	40
3.3.2	As(V) Equilibrium Adsorption in the Absence of Phosphate.....	43
3.3.3	As(V) Equilibrium Adsorption in the Presence of Phosphate.....	46
3.3.4	Overall Reactor Model for As(V) Removal by Electrocoagulation.....	49
3.4	Environmental Implications.....	52
3.5	Acknowledgments.....	53
3.6	Literature Cited.....	53
3.7	Appendix.....	55
Chapter 4	56
4.1	Conclusions.....	56
4.2	Recommendations for Future Work.....	57
Vita	59

List of Tables

Table 2. 1. Experimental variables evaluated in the electrocoagulation experiments	12
Table 2.2. Water compositions in electrocoagulation experiments and the time to achieve dissolved arsenic concentrations below 10 µg/L and 1.0 µg/L	19
Table 2.3. Arsenic removal by the domestic EC units installed at the field sites	29
Table 3.1. Reactions and parameters used for surface complexation modeling of As(V) and phosphate to the lepidocrocite generated from electrocoagulation.....	45
Table 3.2. Parameters used for simulation of the overall electrocoagulation process for treatment of solutions initially containing 100 µg/L As(V).	51

List of Figures

Figure 2.1. Domestic EC setup used for the field study.....	13
Figure 2.2. Concentrations of total and dissolved (a) As(V) and (b) iron during electrocoagulation of a solution initially containing 100 µg/L As(V) at pH 7.0. The dash line in (b) represents the total iron concentration predicted by the Faraday's law at I=0.022 A.	17
Figure 2.3. X-ray diffraction patterns of solids generated during electrocoagulation. The reference pattern for lepidocrocite is included for comparison.	18
Figure 2.4. Dissolved As(V) concentrations during electrocoagulation of solutions initially containing 100 µg/L As(V). The data points for pH 5 are partially obscured by those for pH 6.	20
Figure 2.5. Dissolved concentrations of total As and As(V) during electrocoagulation of solutions initially containing 100 µg/L As(III) at pH 5, 7, and 9.	21
Figure 2.6. Effect of pH on zeta potential of the lepidocrocite suspension generated by electrocoagulation. Measurements were made in the absence of dissolved As, but zeta potential was not affected by As at the concentration studied.	22
Figure 2.7. Relative change in dissolved arsenic during electrocoagulation of solutions initially containing 100 µg/L and 1000 µg/L (a) As(III) and (b) As(V) at pH 7. Panel (a) also shows the concentration of dissolved As(V).	23
Figure 2.8. Dissolved (a) phosphate, (b) dissolved As(V), and (c) total and dissolved iron concentrations during electrocoagulation of solutions initially containing 100 µg/L As(V) at pH 7.	25
Figure 2.9. Dissolved (a) phosphate and (b) As concentrations during electrocoagulation treatment of solutions initially containing 100 µg/L As(III) at pH 7.	26
Figure 2.10. Concentrations of (a) dissolved SiO ₂ , (b) dissolved As(V) and (c) total and dissolved iron concentrations during electrocoagulation of solutions initially containing 100 µg/L As(V) at pH 7.	27
Figure 2.11. Dissolved concentrations of arsenic during electrocoagulation of solutions initially containing (a) 100 µg/L As(V) and (b) 100 µg/L As(III) at pH 7. Panel (b) also shows the concentration of dissolved As(V).	28
Figure 2.12. Domestic EC setup results from the field study. The red arrows indicate the WHO guideline value for arsenic in drinking water (10ppb) and the Indian standards for arsenic in drinking water (50ppb).....	30

Figure 3.1. Concentrations of total and dissolved (a) As(V) at pH 7.0 and (b) iron during electrocoagulation of a solution initially containing 100 $\mu\text{g/L}$ As(V) at pH 5.0 and 7.0. The dashed line in (b) represents the total iron concentration predicted by the Faraday's law at the measured current of 22 mA.	42
Figure 3.2. As(V) adsorption isotherm onto lepidocrocite at pH 4. Data are shown as symbols and simulations are shown as lines. The solid line is the surface complexation model and the dashed line is the Langmuir isotherm.	44
Figure 3.3. As(V) adsorption edges onto lepidocrocite at initial As(V) concentrations of 100 (■) and 1000 $\mu\text{g/L}$ (●). Data are shown as symbols and simulations from the surface complexation model as lines.	46
Figure 3.4. As(V) adsorption edges onto lepidocrocite for 100 $\mu\text{g/L}$ total As(V) in the absence of phosphate (■) and in the presence of 1 (●) and 4 (▲) mg P/L of phosphate. Data are shown as symbols and simulations from the surface complexation model are shown as lines.	47
Figure 3.5. Phosphate adsorption edges onto lepidocrocite in the absence of As(V) and in the presence of 100 $\mu\text{g/L}$ As(V). Data are shown as symbols and simulations from the surface complexation model are shown as lines.	48
Figure 3.6. Electrocoagulation of solutions initially containing 100 $\mu\text{g/L}$ As(V) at pH 5, 7 and 9. Data are shown as symbols and simulations are shown as lines. Data and simulations at pH 5 are partially obscured by those at pH 7.	51

Chapter 1

Introduction

1.1 Background

Arsenic occurs in groundwater primarily as the result of natural weathering of arsenic-containing rocks, although in certain areas, high arsenic concentrations are caused by industrial waste discharges and application of arsenical herbicides and pesticides (Jain and Ali, 2000). Arsenic contamination of groundwater is found in both the developed and developing countries. Arsenic is a carcinogen and its consumption can negatively affect the gastrointestinal tract and cardiac, vascular and central nervous systems.

Exposure to arsenic through drinking water is a great threat to human health.

Considering the high toxicity of arsenic, the World Health Organization (WHO) and USEPA set a maximum acceptable level of arsenic in drinking water at 10 $\mu\text{g/L}$ (USEPA, 2002; WHO, 1993).

Iron oxides have been widely used as sorbents for arsenic removal. They usually have strong adsorption affinities for arsenic and they can have large specific surface areas (Dixit and Hering, 2003). Iron oxides have been used in different forms for arsenic removal. It has been reported for arsenic removal either in the form of iron oxide suspensions (Dixit and Hering, 2003), packed beds of iron oxides (Zeng et al., 2008a), conventional chemical coagulation (Meng et al., 2000) or electrocoagulation using iron electrodes (Kumar et al., 2004).

Arsenic is present in water and wastewater mainly in the forms of arsenate (As(V)) and arsenite (As(III)). In the environmentally relevant pH range of 4-10, the dominant As(V) species are negatively charged (H_2AsO_4^- and HAsO_4^{2-}), while the dominant As(III) species are neutrally charged (H_3AsO_3). The negatively charged As(V) species are more likely to be adsorbed and are generally more easily removed. In treatment systems As(V) is removed more efficiently than As(III) (Balasubramanian and Madhavan, 2001; Kumar et al., 2004; Parga et al., 2005).

The adsorption of arsenate to iron oxides is affected by pH because of the variation in the surface charge of the iron oxides and the speciation of arsenate with pH. In the environmentally relevant pH range of 4-10, the dominant As(V) species are negatively charged. The surface potential of the iron oxides, as measured by zeta potential, is positive below about pH 7 and negative above this pH. For an interfacial double layer, the zeta potential is the electric potential between the slipping plane and the bulk fluid away from the interface. A zero zeta potential is interpreted as the point of zero net charge at a surface. This is referred to as the isoelectric point (IEP). In other words, the IEP is the pH at which a surface shows no net electrical charge. The point of zero charge (PZC) is often used to approximate the IEP (Maurice, 2009). Below the IEP the surfaces of the iron oxides are positively charged and electrostatic contributions as well as chemical contributions contribute to As(V) adsorption. Above the IEP, both the As(V) species and the surface of iron oxide is negatively charged and adsorption is less favorable due to electrostatic repulsion.

Electrocoagulation is an emerging water and wastewater treatment technology that involves electrolytic oxidation of an anode material and in situ generation of

coagulant (Kumar et al., 2004; Lakshmanan et al., 2009). When a current is applied between two electrodes, metal ions such as Fe^{2+} and Al^{3+} that can contribute to coagulant formation are released by anode oxidation. The Fe^{2+} can subsequently be oxidized in solution to produce an Fe(III) hydroxide or oxyhydroxide (Lakshmanan et al., 2009). Electrocoagulation is an alternative to using chemical coagulants for arsenic removal; thus it can be beneficial for communities with better access to electricity than to chemicals. So far, several studies have reported arsenic removal from water and wastewater by electrocoagulation (Balasubramanian and Madhavan, 2001; Kumar et al., 2004; Parga et al., 2005). During such processes, arsenic removal by electrocoagulation involved metal oxide formation followed by arsenic removal (Balasubramanian and Madhavan, 2001). In addition, electrocoagulation may also control oxidation-reduction reactions; species such as As(III) may be oxidized on the anode and other species may be reduced on the cathode.

Several water chemistry factors may affect arsenic removal by electrocoagulation. The pH of the water influences arsenic removal by electrocoagulation by affecting arsenic species distribution, the surface charge of the metal oxides formed during electrocoagulation, and the rate of Fe(III) production from the Fe(II) released from the iron anode (Kumar et al., 2004; Lakshmanan et al., 2009). As(V) adsorption decreases with increasing pH, and Fe(II) oxidation is faster at high pH (Lakshmanan et al., 2009). Surface complexation models (SCM) have been used successfully to describe the pH dependence of As(V) adsorption onto iron oxides (Dixit and Hering, 2003; Wilkie and Hering, 1996; Zeng et al., 2008b). Because phosphate and arsenic are in the same group and arsenate and phosphate have similar chemical properties, they may have similar

affinity to the iron oxides and can compete for the surface sites on the iron oxides. The competition of As(V) and phosphate for adsorption onto iron oxide-based sorbent by the presence of phosphate were also simulated successfully by surface complexation models (Holm, 2002; Zeng et al., 2008b). Silica can be present at high concentrations in groundwater, and in studies with iron-oxide based sorbents has been observed to inhibit arsenic removal (Davis et al., 2001; Zeng et al., 2008a).

During surface complexation modeling, the ion distribution can be computed as follows. First, the equilibrium speciation of the surface is determined using mole balance equations and the surface complexation and aqueous phase reactions. From the surface speciation, the surface charge density at the surface is calculated. In the diffuse double layer model, the surface potential is then calculated from the surface charge density using Gouy-Chapman theory. The surface potential is then used to modify the effective equilibrium surface complexation constants from the intrinsic equilibrium constants. The adsorption of ions can be recomputed using the modified equilibrium constants. By iterating this whole computation process, the optimal conditions that can simultaneously satisfy all the equations governing the system can eventually be identified (Benjamin, 2002).

1.2 Objectives

The primary objective of this study was to assess the impact of important water chemistry factors on arsenic removal by electrocoagulation. Factors studied were the pH, arsenic oxidation state, initial arsenic concentration, and presence of dissolved phosphate, silica and sulfate. In pursuing this objective, additional objectives were to: investigate the

effects of water chemistry on As(V) adsorption to the iron oxides generated by electrocoagulation, and develop a surface complexation model to simulate As(V) equilibrium adsorption. A secondary objective of this study was to prepare an overall model for the performance of an electrocoagulation system for As(V) removal.

1.3 References

- Balasubramanian, N., Madhavan, K., 2001. Arsenic removal from industrial effluent through electrocoagulation. *Chemical Engineering and Technology*, 24, 519-521.
- Benjamin, M.M., 2002. *Water Chemistry*. McGraw-Hill, New York.
- Davis, C.C., Knocke, W.R., 2001. Edwards M. Implications of aqueous silica sorption to iron hydroxide: Mobilization of iron colloids and interference with sorption of arsenate and humic substances. *Environmental Science & Technology* , 35, 3158-3162.
- Dixit, S., Hering, J. G., 2003. Comparison of arsenic(V) and arsenic(III) sorption onto iron oxide minerals: Implications for arsenic mobility. *Environmental Science & Technology*, 37, 4182-4189.
- Holm, T.R., 2002. Effects of CO_3^{2-} /bicarbonate, Si, and PO_4^{3-} on arsenic sorption to HFO. *Journal American Water Works Association*, 94, 174-181.
- Jain, C.K., Ali, I., 2000. Arsenic: occurrence, toxicity and speciation techniques. *Water Research*, 34, 4304-4312.
- Kumar, P.R., Chaudhari, S., Khilar, K.C., Mahajan, S. P., 2004. Removal of arsenic from water by electrocoagulation. *Chemosphere*, 55, 1245-1252.
- Lakshmanan, D., Clifford, D.A., Samanta, G., 2009. Ferrous and ferric ion generation during iron electrocoagulation. *Environmental Science and Technology*, 43, 3853-3859.
- Maurice P. A., 2009. *Environmental surfaces and interfaces from the nanoscale to the global scale*. John Wiley & Sons, NJ.
- Meng, X.G., Bang, S., Korfiatis, G.P., 2000. Effects of silicate, sulfate, and carbonate on arsenic removal by ferric chloride. *Water Research*, 34, 1255-1261.
- Parga, J.R., Cocke, D.L., Valenzuela, J.L., Gomes, J.A., Kesmez, M., Irwin, G., Moreno, H., Weir, M., 2005. Arsenic removal via electrocoagulation from heavy metal contaminated groundwater in La Comarca Lagunera Mexico. *Journal of Hazardous Materials*, 124: 247-254.

United States Environmental Protection Agency,2002. Implementation guidance for the arsenic rule--drinking water regulations for arsenic and clarifications to compliance and new source contaminants monitoring. EPA/816/K-02/018. U.S. EPA Office of Water, Washington,DC.

Wilkie, J.A., Hering, J.G.,1996. Adsorption of arsenic onto hydrous ferric oxide: Effects of adsorbate/adsorbent ratios and co-occurring solutes. *Colloids and Surfaces A-Physicochemical and Engineering Aspects*,107, 97-110.

World Health Organization,1993. Guidelines for drinking water quality: Remediations, vol. 1 (3rd ed.). Geneva: WHO.

Zeng, H., Arashiro, M., Giammar, D.E., 2008a. Effects of water chemistry and flow rate on arsenate removal by adsorption to an iron oxide-based sorbent. *Water Research*, 42, 4629-4636.

Zeng, H., Fisher, B., Giammar, D.E.,2008b. Individual and competitive adsorption of arsenate and phosphate to a high-surface-area iron oxide-based sorbent. *Environmental Science and Technology*, 42, 147-152.

Chapter 2

Effects of Water Chemistry on Arsenic Removal from Drinking Water by Electrocoagulation

(The field work presented in this chapter was done by collaborators at Indian Institute of Technology Bombay)

This chapter is a manuscript in preparation for submission to *Water Research*

Abstract: Exposure to arsenic through drinking water poses a threat to human health. Electrocoagulation is an emerging water treatment technology that involves electrolytic oxidation of anode materials and *in-situ* generation of coagulant. The electrochemical generation of coagulant is an alternative to using chemical coagulants, and the process can also oxidize As(III) to As(V). Batch electrocoagulation experiments were performed in the laboratory using iron electrodes. The experiments quantified the effects of pH, initial arsenic concentration and oxidization state, and concentrations of dissolved phosphate, silica and sulfate on the rate and extent of arsenic removal. The iron generated during electrocoagulation precipitated as lepidocrocite (γ -FeOOH), except when dissolved silica was present, and arsenic was removed by adsorption to the lepidocrocite. Arsenic removal was slower at higher pH. When solutions initially contained As(III), a portion of the As(III) was oxidized to As(V) during electrocoagulation. As(V) removal was faster than As(III) removal. The presence of 1 and 4 mg/L phosphate inhibited arsenic removal, while the presence of 5 and 20 mg/L silica or 10 and 50 mg/L sulfate had no significant effect on arsenic removal. For most conditions examined in this study, over 99% arsenic removal efficiency was achieved. Effective arsenic removal was also demonstrated in a field deployment of household electrocoagulation systems in Eastern India.

Keywords: Arsenic, water treatment, electrocoagulation, phosphate, adsorption, lepidocrocite

2.1 Introduction

Exposure to arsenic through drinking water is a great threat to human health (Jain and Ali, 2000). Arsenic is a carcinogen and its consumption can negatively affect the gastrointestinal tract and cardiac, vascular and central nervous systems. Considering the high toxicity of arsenic, the World Health Organization (WHO) and USEPA set the maximum acceptable level of arsenic in drinking water at 10 µg/L (USEPA, 2002; WHO, 1993). Arsenic occurs in groundwater primarily as the result of natural weathering of arsenic containing rocks, although in certain areas, high arsenic concentrations are caused by industrial waste discharges and application of arsenical herbicides and pesticides (Jain and Ali, 2000).

Iron oxides have been widely used as sorbents for arsenic removal. They usually have strong adsorption affinities for arsenic and they can have large specific surface areas (Dixit and Hering, 2003). Arsenic is present in water and wastewater mainly in the forms of arsenate (As(V)) and arsenite (As(III)). In the environmentally relevant pH range of 4-10, the dominant As(V) species are negatively charged (H_2AsO_4^- and HAsO_4^{2-}), while the dominant As(III) species is neutrally charged (H_3AsO_3). The negatively charged As(V) species are more likely to be adsorbed and are generally more easily removed than As(III) in treatment systems (Balasubramanian and Madhavan, 2001; Kumar et al., 2004; Parga et al., 2005).

Electrocoagulation is an emerging water and wastewater treatment technology that involves electrolytic oxidation of an appropriate anode material and *in-situ* generation of coagulant (Kumar et al., 2004; Lakshmanan et al., 2009). When a direct

current is applied between two electrodes, metal ions such as Fe^{2+} and Al^{3+} that can contribute to coagulant formation are released by anode oxidation. With iron electrodes, the Fe^{2+} released can subsequently be oxidized in solution to produce an Fe(III) hydroxide or oxyhydroxide (Lakshmanan et al., 2009). Electrocoagulation is an alternative to using chemical coagulants for arsenic removal and thus is beneficial for communities with better access to electricity than to chemicals. Several previous studies have reported arsenic removal from water and wastewater by electrocoagulation (Balasubramanian and Madhavan, 2001; Kumar et al., 2004; Parga et al., 2005; Thella et al., 2008). During such processes, arsenic removal by electrocoagulation involved metal oxide formation followed by arsenic removal (Balasubramanian and Madhavan, 2001). Electrocoagulation may also control oxidation-reduction reactions; species such as As(III) may be oxidized on the anode and other species may be reduced on the cathode.

Several water chemistry factors may affect arsenic removal by electrocoagulation. The pH can affect arsenic species distribution and the surface charge of the metal oxides formed. Arsenic oxidation state can affect arsenic removal, with As(V) being more easily removed than As(III) (Kumar et al., 2004). Phosphate may compete with arsenic for adsorption sites (Meng et al., 2002). Silica can be present at high concentration in groundwater, and in studies with iron oxide-based sorbents has been observed to inhibit arsenic removal (Davis et al., 2001; Zeng et al., 2008a).

The objectives of this study were to assess the impact of important water chemistry factors on arsenic removal by electrocoagulation and to examine the performance of electrocoagulation for arsenic removal in laboratory and field settings.

Factors studied were the pH, arsenic oxidization state, initial arsenic concentration, and the concentrations of dissolved phosphate, silica, and sulfate.

2.2 Materials and Methods

2.2.1 Laboratory-scale Electrocoagulation Experiments

The electrocoagulation reactor consisted of a 1 L glass beaker with two iron rods immersed in the aqueous solution. The rods had diameters of 1.75 cm, lengths of 20 cm, and were placed 2 cm apart in the arsenic containing solution. The total submerged surface area of each electrode was 57 cm². Before each experiment, the electrodes were abraded with sand paper to remove scales and then cleaned with 1 M HNO₃ and ultrapure water. A direct current was applied at 22 mA to the terminal electrodes from a direct current power supply set at a voltage of 12 V. The electric current was monitored over the course of each two hour experiment. To provide enough oxygen for the formation of Fe(III) precipitates, the solution was sparged with air at a flow rate of 60 mL/min. The arsenic containing solution was magnetically-stirred (200 rpm). Duplicate runs were carried out for each set of experimental conditions.

The water compositions evaluated are listed in Table 2.1. All solutions were prepared with ultrapure water. To prepare each solution for electrocoagulation experiments, desired volumes of stock solutions were added to the 1 L glass beaker. An As(V) stock solution was made from Na₂HAsO₄·7H₂O. The As(III) stock solution was made from NaAsO₂. Tests indicated that the stock As(III) solution contained about 15% As(V). The phosphate, silica, and sulfate stock solutions were made from Na₂HPO₄·7H₂O, Na₂SiO₃·9H₂O, and Na₂SO₄·10H₂O, respectively. In order to provide

pH buffering, NaHCO₃ was added to achieve a concentration of 1 mM. The pH of the As-containing solution in each beaker was periodically readjusted to the target value by adding aliquots of 1 M HNO₃ or 1 M NaOH.

Table 2. 1. Experimental variables evaluated in the electrocoagulation experiments

Parameters	Range of values
Initial arsenic concentration	100 and 1000 µg/L
Arsenic oxidization state	As(III) and As(V)
pH	5, 6, 7, 8 and 9
Phosphate	0, 1 and 4 mg/L as P
Silica	0, 5 and 20 mg/L as SiO ₂
Sulfate	0, 10 and 50 mg/L as SO ₄ ²⁻

For the experiments using As(V), every 5, 15 or 30 min, 15 mL of solution was collected from the beaker. Of this amount, 7.5 mL was filtered using a 0.45 µm filter membrane (polyethersulfone), and the filtrate was acidified to 1% HNO₃. Another 7.5 mL of unfiltered suspension was acidified to 1% HNO₃ by addition of concentrated HNO₃, which completely dissolved the suspended solids. For the experiments using As(III), an additional sample was collected for arsenic redox speciation (i.e. separation of As(III) and As(V)) using an anion-exchange method (Wilkie,1997). Before separation, the pH of a 10 mL aliquot of filtered solution was adjusted to around 3.5 and then passed through a column containing anion exchange resin. During As separation, the first 5 mL of solution were wasted and the remaining 5 mL were collected. In this method, As(III) eluted through the column and As(V) was retained on the resin in the column. At the end of each experiment, 15 mL of unfiltered suspension was collected for zeta potential measurement. The remaining settleable solids were collected and freeze-dried in preparation for solid-phase characterization.

The pH of the solution in the beaker was measured with a pH electrode when the current was not applied because the current interfered with the pH measurement. It took approximately 1 min to adjust the pH to the desired value. Considering the time used to adjust the pH, each experiment lasted about 130 min, although current was only applied during 120 minutes of the experiment.

2.2.2 Materials and Methods of the Field Study

EC setup used for the field studies consist of a bucket of volume 50L, a 12V D.C. source of rating 2A, iron plates of size 10cm by 15cm with a submerged depth of 10cm and an aquarium pump with diffuser. The electrodes are separated by a distance of 0.5cm and are connected to the support by a non conducting PVC screw. This setup is followed by a common candle filter assembly (Figure 2.1).

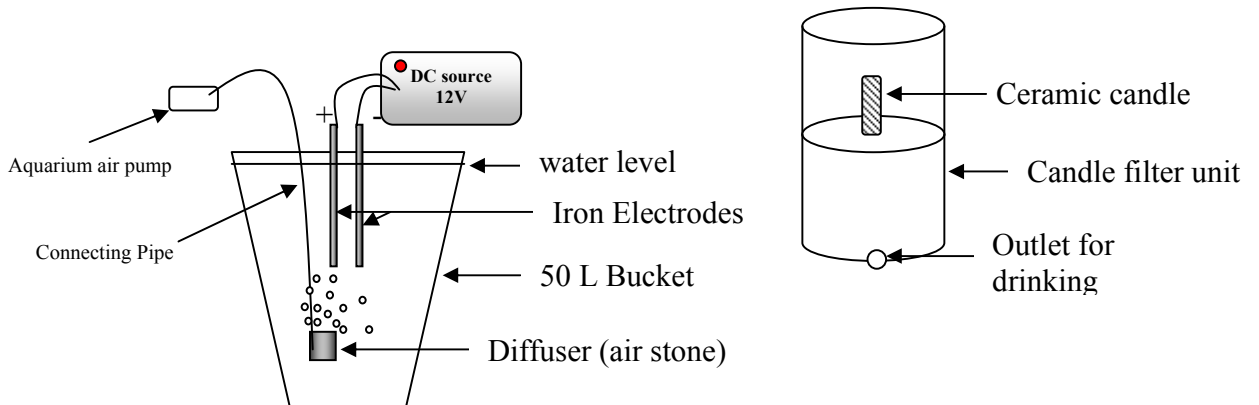


Figure 2.1. Domestic EC setup used for the field study

Field trials for the EC setup were carried out in locations in the Nadia district of West Bengal. We carried out the field trials in two villages in this district. The first village, Lalmath, falls under the Krishnanagar II Block. It has a population of 500

families and all the families have at least one or two family members suffering from arsenicosis or other related health effects. Average concentration of Arsenic in the groundwater was reported to be 700ppb. The second village was Ghetugachi, which falls under Chakdaha block. This village has more than 650 families. The average arsenic levels in this village were reported to be 400ppb. But here it was mostly As(III) form of arsenic. Also the phosphate levels in the groundwater were substantially higher. So the waters of these villages can be termed as difficult waters. 17 EC setups were distributed in Ghetugachi and one was set up in Lalmath. 50L water was collected in the bucket from the handpumps located close to the house where the EC setups had been installed. The aquarium pump is switched on for 15 minutes to allow the DO in the water to increase to over 3mg/L, to ensure the formation of Hydrous Ferric Oxide (HFO), which forms only in high DO conditions. The electrode assembly is then immersed in the water and EC is carried out for 3 hrs. After this the water is allowed to settle for 4 hrs. The supernatant of this stagnant water is collected and filtered through a local ceramic candle filter. Water samples collected are as follows:

- from the raw water before the aquarium pump is switched on
- from the supernatant of the treated water after 4hrs of settling
- and after candle filtration.

After collection the water samples were preserved in acidic condition. Then the samples were brought to the lab and analyzed for arsenic, iron and phosphate concentrations.

2.2.3 Analysis Methods

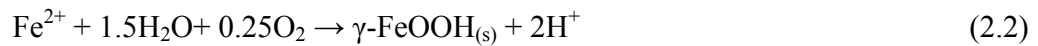
The filtered and acid-treated samples were analyzed for dissolved and total concentrations of constituents, respectively. The concentrations of As, Fe, P and Si were determined by inductively coupled plasma mass spectrometry (ICP-MS) (7500ce, Agilent Technologies, Santa Clara, CA). The instrument detection limits for As, Fe, P and Si were 0.1 µg/L, 0.05 mg/L, 0.01 mg/L, and 0.03 mg/L, respectively. The specific surface areas (SSA) of the solids were measured by the BET (Brunauer-Emmett-Teller) N₂-adsorption method (Autosorb-1-C, Quantachrome, U.S.A.). X-ray powder diffraction (XRD) patterns were collected using Cu K α radiation (D-MAX/A, Rigaku, Japan). Zeta potential was measured by a nanoparticle characterization instrument with zeta potential capability (Nanoseries ZS, Malvern Instruments, U.K.). Dissolved oxygen for selected samples was measured using a Hach Surface Water Test Kit (Fondriest Environmental, Inc.).

The analysis of the field samples were carried out by spectroscopic methods. Arsenic concentration in the field samples was determined using a rapid colorimetric method (Dhar et al., 2004). The iron concentration in the field samples was determined using phenanthroline method [APHA]. Random samples were then analysed with an AAS (AA 400-FIAS, Perkin Elmer, USA) to verify the iron and arsenic concentrations. Error of the spectrophotometric method was seen to be $\pm 2.0\%$, which is considered negligible. The phosphate concentration in the field samples was determined using ascorbic acid method [APHA].

2.3 Results and discussion

2.3.1 Production of Iron Oxide Coagulant

During the electrocoagulation process, the solutions changed from colorless to reddish brown. The concentrations of the total iron generated during electrocoagulation increased linearly with reaction time (Figure 2.2). In this study, the reported values are the average plus the standard deviation. For all the electrocoagulation experiments, about 50 mg/L (average value was 50.5 mg/L) total iron was produced over the 2 hour experiment duration. The reactor was operated with a current of 22 mA, and the total iron produced was consistent with a value of 52.2 mg/L predicted by Faraday's Law for the oxidation of the iron electrode to dissolved Fe(II). Fe was released to solution as Fe(II) and was then oxidized to Fe(III) by the dissolved oxygen. The Fe(III) then precipitated in the formation of iron oxides (Reactions 2.1 and 2.2). At the cathode hydrogen gas is generated from the reduction of water (Reaction 2.3).



For the experiment using 100 µg/L As(V) at pH 7, samples were collected at 30, 60 and 90 min, and the dissolved oxygen (DO) was around 10 mg/L, which indicated that the solution was saturated with dissolved oxygen. The DO at 25°C predicted from Henry's law is 8.7 mg/L. The dissolved iron concentrations were very low compared with

the total iron concentrations in each experiment, which indicated that nearly all of the iron was present in the solid phases.

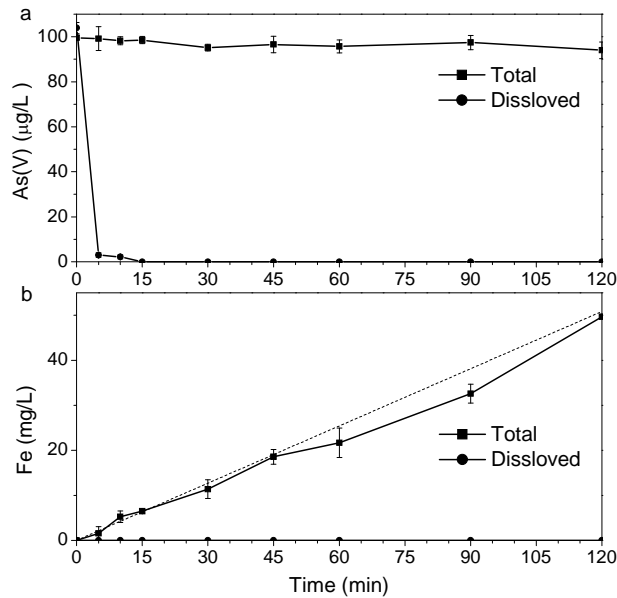


Figure 2.2. Concentrations of total and dissolved (a) As(V) and (b) iron during electrocoagulation of a solution initially containing 100 µg/L As(V) at pH 7.0. The dash line in (b) represents the total iron concentration predicted by the Faraday's law at I=0.022 A.

The Fe(III) solid was identified as lepidocrocite (γ -FeOOH) by its XRD pattern (Figure 2.3). The identity of the iron oxyhydroxides formed was not affected by As(III) and As(V) or by the presence of sulfate or phosphate. The XRD pattern at pH 5 had no clear XRD peaks, probably resulting from the insufficient solids collected for XRD characterization. The specific surface area of the solids was 200.5 m²/g and was independent of the solution compositions. The formation of lepidocrocite is consistent with published synthesis methods involving oxidation of Fe(II) solutions using dissolved oxygen at ambient temperature (Schwertmann and Cornell, 2000). The rate of Fe(II)

oxidation increases with increasing pH (Stumm and Morgan, 1996), and a previous electrocoagulation study confirmed that Fe(II) oxidation by dissolved oxygen was slower at lower pH (Lakshmanan et al., 2009). The presence of silica significantly affected the iron oxides formed during electrocoagulation (Figure 2.3). Less crystalline iron oxides were formed in the presence of silica. A previous study found that silica influenced the type of iron oxides formed in aerated Fe(II)- and As(III)-containing water by decreasing the degree of corner-sharing linkages of Fe(III)-octahedra during Fe(III) polymerization (Voegelin et al., 2010). Equilibrium calculations indicate that Fe(III) oxyhydroxides should precipitate at the experimental conditions and that no arsenic-Fe(III) precipitates (e.g. $\text{FeAsO}_4(s)$) were expected to form.

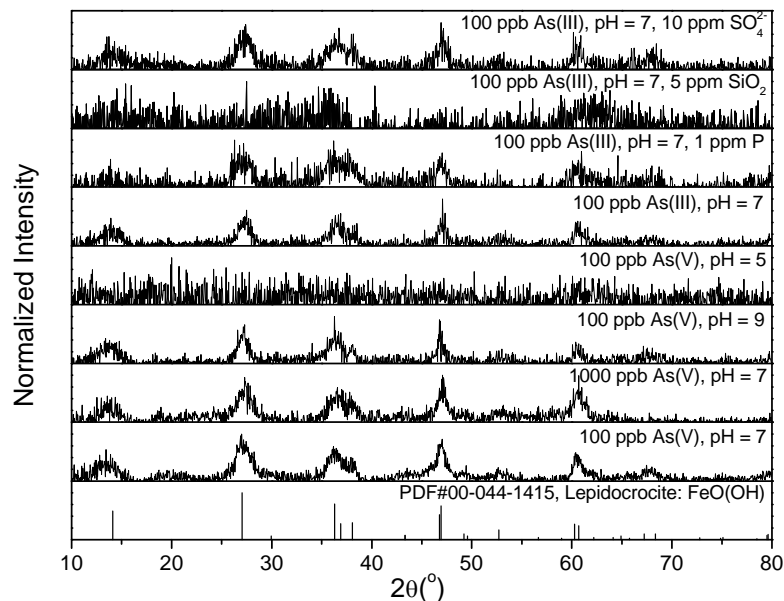


Figure 2.3. X-ray diffraction patterns of solids generated during electrocoagulation. The reference pattern for lepidocrocite is included for comparison.

2.3.2 Effect of pH on As Removal

The removal rate of arsenic was affected by the pH. For experiments using 100 µg/L As(V), it took less than 30 min for the dissolved As(V) concentrations to drop below 1 µg/L at pH 5, 6 and 7 (Table 2.2).

Table 2.2. Water compositions in electrocoagulation experiments and the time to achieve dissolved arsenic concentrations below 10 µg/L and 1.0 µg/L

Arsenic oxidation state	Arsenic (µg/L)	pH	Phosphate as P (mg/L)	Silica as SiO ₂ (mg/L)	Sulfate as SO ₄ ²⁻ (mg/L)	Time to dissolved As < 10 µg/L (min)	Time to dissolved As < 1.0 µg/L (min)
As(III)	100	5	0	0	0	30	90
As(III)	100	6	0	0	0	30	90
As(III)	100	7	0	0	0	30	90
As(III)	100	8	0	0	0	30	90
As(III)	100	9	0	0	0	45	90
As(III)	1000	7	0	0	0	90	120
As(V)	1000	7	0	0	0	45	>120
As(V) *	100	5	0	0	0	15	15
As(V) *	100	6	0	0	0	15	30
As(V)	100	7	0	0	0	5	15
As(V) *	100	8	0	0	0	75	75
As(V) *	100	9	0	0	0	75	>120
As(V)	100	7	1	0	0	60	>120
As(V)	100	7	4	0	0	90	>120
As(V)	100	7	0	5	0	5	60
As(V)	100	7	0	20	0	5	60
As(V)	100	7	0	0	10	5	30
As(V)	100	7	0	0	50	5	45
As(III)	100	7	1	0	0	45	90
As(III)	100	7	0	5	0	30	90
As(III)	100	7	0	0	10	30	90

*The first sample was collected after 15 min in these experiments but after 5 min in all other experiments.

At pH 8, the dissolved As(V) concentration only reached this value after 75 min, and at pH 9 the dissolved As(V) concentrations remained at 4 $\mu\text{g/L}$ after 120 min (Figure 2.4). For experiments using 100 $\mu\text{g/L}$ As(III), it took 90 min for the dissolved As concentrations to drop below 1 $\mu\text{g/L}$ at pH 5-8, and at pH 9 it took 120 min (Figure 2.5 and Table 2.2). Although As removal was slower at higher pH, the final removal efficiency was independent of pH from 5 to 8. Once sufficient lepidocrocite was produced to provide adsorption sites for As, low dissolved As concentrations could be obtained. Kumar et al. (2004) also reported that the final As removal efficiency was independent of pH with increasing pH from 6 to 8 during electrocoagulation.

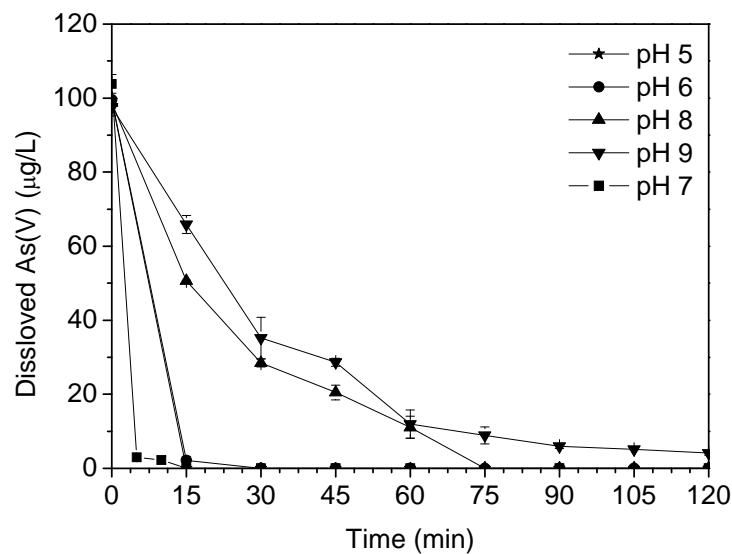


Figure 2.4. Dissolved As(V) concentrations during electrocoagulation of solutions initially containing 100 $\mu\text{g/L}$ As(V). The data points for pH 5 are partially obscured by those for pH 6.

The influence of pH on adsorption can explain the slower rate of As(V) removal with increasing pH. The pH-dependence of As(V) and As(III) adsorption to lepidocrocite formed during electrocoagulation is in agreement with the effect of pH on As adsorption to hydrous ferric oxide and goethite (Dixit and Hering, 2003; Meng et al., 2000). The lepidocrocite produced in the electrocoagulation reactor had a measured point-of-zero-charge pH (PZC) of about 7.0 (Figure 2.6), which is comparable with that reported by Peacock and Sherman (2004) using a potentiometric titration method. Below this pH the surfaces of the particles are positively charged and electrostatic contributions as well as chemical contributions contribute to As(V) adsorption. Above the PZC, both the As(V) species and the lepidocrocite surface are negatively charged and adsorption is less favorable.

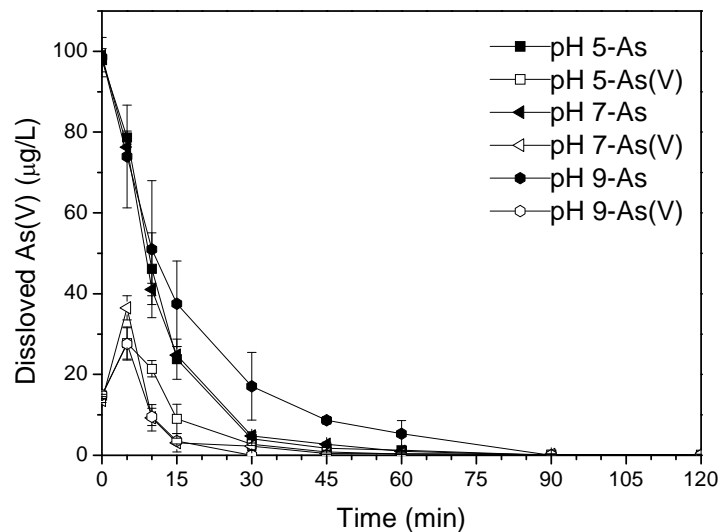


Figure 2.5. Dissolved concentrations of total As and As(V) during electrocoagulation of solutions initially containing 100 µg/L As(III) at pH 5, 7, and 9.

At pH 9, the removal of As(V) was slower than As(III) (Figures 2.4 and 2.5). One possible reason for this observation was that at pH 9 the lepidocrocite surface is negatively charged and part of the As(III) species are neutrally charged, but the As(V) species were negatively charged; thus, electrostatic repulsion cannot hinder As(III) adsorption to lepidocrocite as much as it can As(V) adsorption.

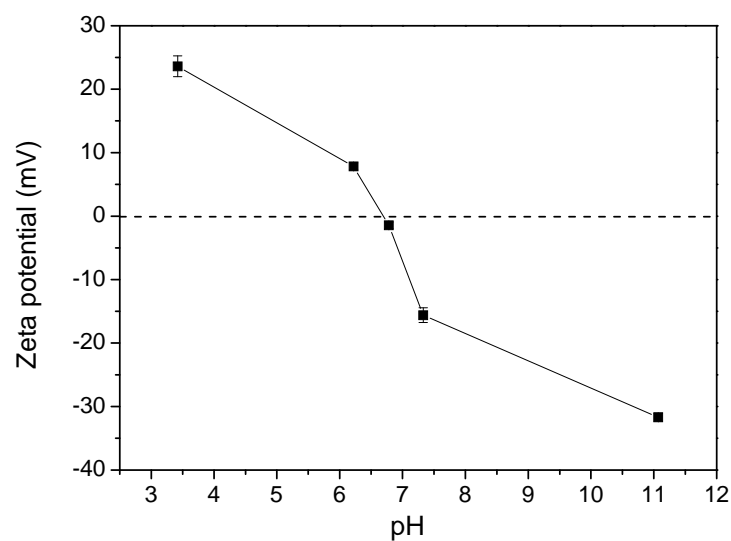


Figure 2.6. Effect of pH on zeta potential of the lepidocrocite suspension generated by electrocoagulation. Measurements were made in the absence of dissolved As, but zeta potential was not affected by As at the concentration studied.

2.3.3 Effect of Oxidation State on As Removal

As(V) removal was usually faster than As(III) removal (Figures 2.4 and 2.5). This was in agreement with the results reported by Kumar et al. (2004) for electrocoagulation and the results reported by Meng et al. (2004) for arsenic adsorption to iron hydroxides. In all the experiments using As(III), the dissolved As(V) concentration increased first and then

decreased with increasing reaction time. The increase in As(V) when treating As(III) solutions indicated that at least 25% As(III) was oxidized to As(V) during electrocoagulation (Figure 2.5).

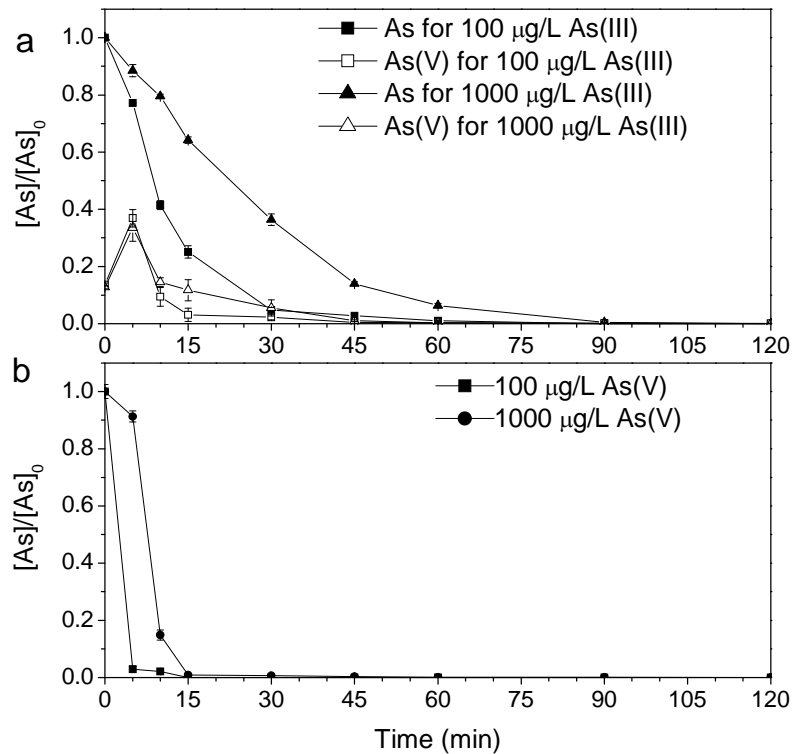


Figure 2.7. Relative change in dissolved arsenic during electrocoagulation of solutions initially containing 100 $\mu\text{g/L}$ and 1000 $\mu\text{g/L}$ (a) As(III) and (b) As(V) at pH 7. Panel (a) also shows the concentration of dissolved As(V).

The removal mechanism for As(III) by electrocoagulation was proposed to be the oxidation of As(III) to As(V) followed by adsorption onto the iron oxides generated (Kumar et al., 2004). As(III) oxidation to As(V) has previously been proposed to occur with dissolved oxygen as the oxidant and intermediate iron-containing species as rate-enhancing species (Ciardelli et al., 2008; Sahai et al., 2007). As(III) oxidation can also occur when Fe(II) is present with Fe(III) oxyhydroxides, and the mechanism has been

proposed to involve the formation of an Fe(IV) intermediate (Amstaetter et al., 2010; Bisceglia et al., 2005).

2.3.4 Effect of Initial As Concentrations on As Removal

As(V) and As(III) removal to below 1 µg/L took more time when the solutions had higher initial As concentrations (Figure 2.7 and Table 2.2). When the initial arsenic concentrations were higher, more iron oxides were needed to decrease the dissolved arsenic concentrations. Arsenic removal is consequently limited by the production rate of lepidocrocite. However, the final As removal efficiencies were independent of the initial As(III) concentration and were over 99%. This was in agreement with the results of Kumar et al. (2004).

2.3.5 Effect of Phosphate on As Removal

The presence of 1 mg/L and 4 mg/L phosphate as P inhibited the removal of As (Figures 2.8 and 2.9). The inhibitory effect was more significant at higher phosphate concentrations. Considerable phosphate was also removed during the electrocoagulation (Figures 2.8 and 2.9). These results indicate that phosphate can compete with As species for the surface sites of lepidocrocite and decrease As adsorption. A competition adsorption effect of phosphate on As removal agreed with the results of previous studies (Meng et al., 2002; Zeng et al., 2008b). The inhibitory effect of phosphate on As removal by electrocoagulation may also be caused by the slower oxidization of Fe(II) to Fe(III) in the presence of phosphate, which can decrease the rate at which the sorbent is formed (Figure 2.8c).

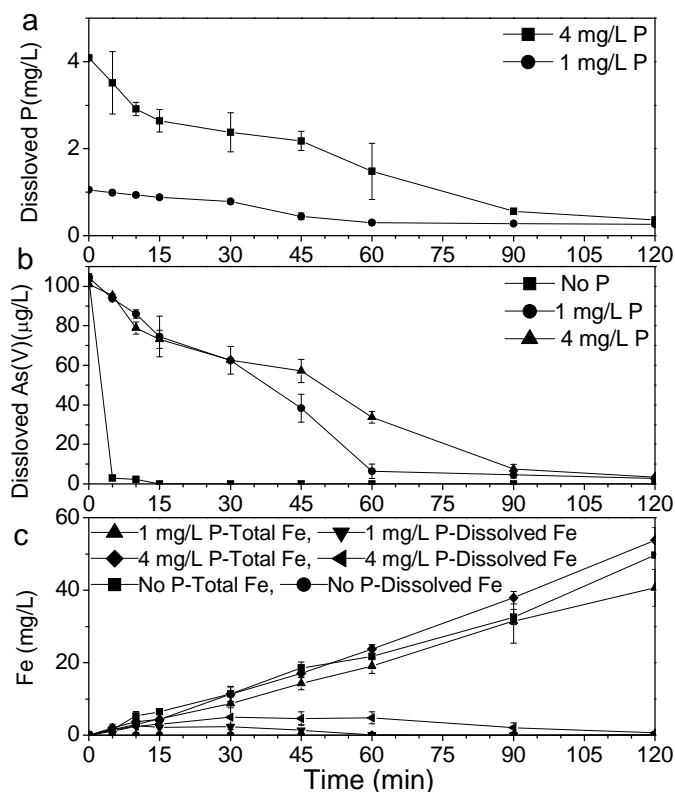


Figure 2.8. Dissolved (a) phosphate, (b) dissolved As(V), and (c) total and dissolved iron concentrations during electrocoagulation of solutions initially containing 100 µg/L As(V) at pH 7.

Recent work has observed formation of Fe(III)-phosphate solids during the oxidation of Fe(II) in phosphate-rich solids (Figure 2.8c) (Voegelin et al., 2010); however, in the present study phosphate did not affect the identity of the iron oxide formed during electrocoagulation (Figure 2.3). Lepidocrocite was the only phase indicated in XRD patterns, and there were no peaks for Fe(II) or Fe(III) phosphate solids.

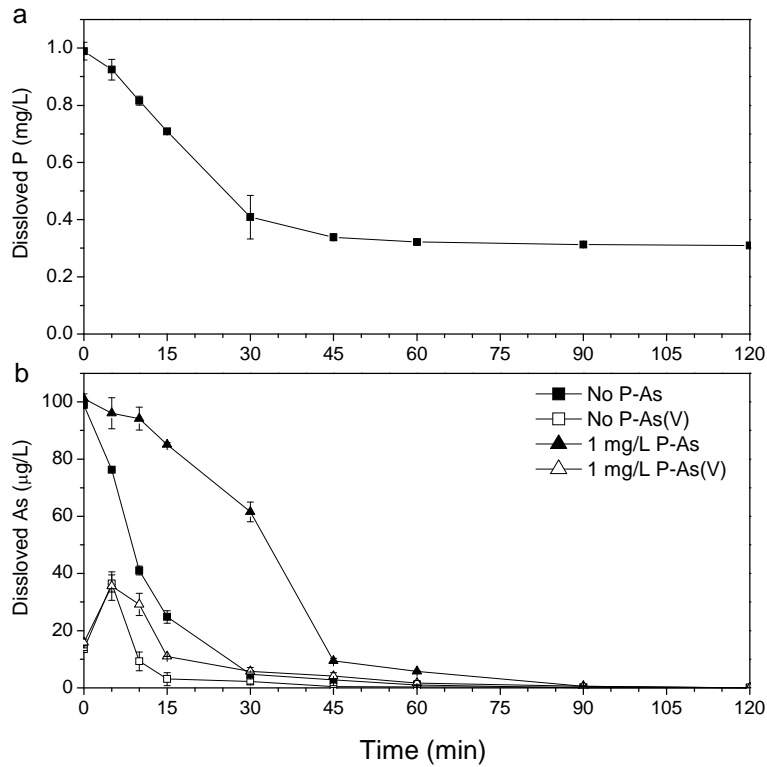


Figure 2.9. Dissolved (a) phosphate and (b) As concentrations during electrocoagulation treatment of solutions initially containing 100 µg/L As(III) at pH 7.

2.3.6 Effect of Silica on As Removal

The presence of 5 and 20 mg/L dissolved SiO₂ had no significant effects on As removal, even though considerable silica was also removed during the electrocoagulation process (Figure 2.10) and silica prevented the formation of lepidocrocite (Figure 2.3). Meng et al. (2002) also observed no significant effects of SiO₂ on As(V) adsorption to iron hydroxides when SiO₂ was present at concentrations as high as 36 mg/L. In a separate study, Davis et al. (2001) observed dissolved SiO₂ inhibition of As(V) adsorption to ferric hydroxide, but only when silica and ferric hydroxide had been pre-equilibrated for 50 days; at shorter contact times, there was much less inhibition. In contrast to the lack of

inhibitory effects of silica in the present study, Zeng et al.(2008a) observed inhibitory effects of 20 mg/L SiO_2 on As(V) removal in column experiments at pH 7.5 using an iron oxide-based sorbent.

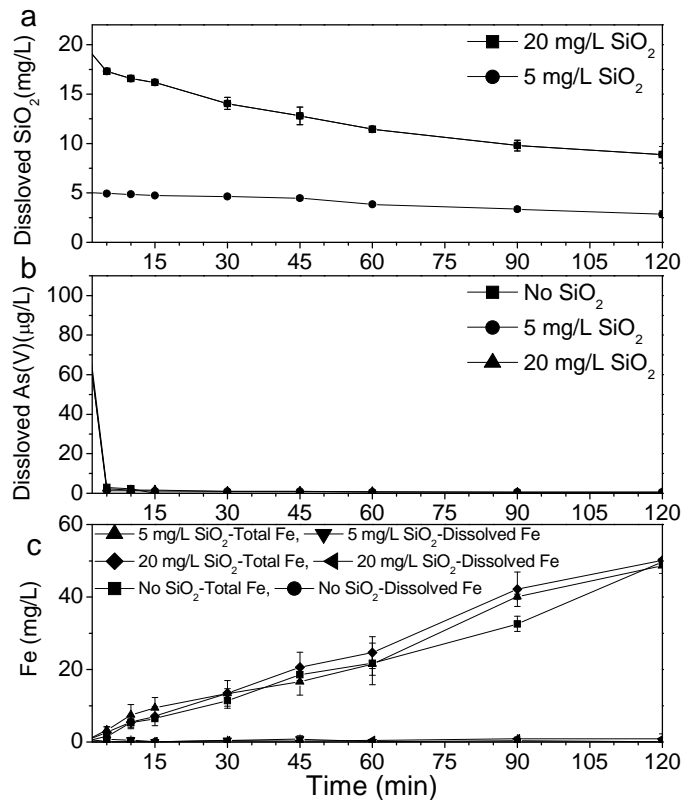


Figure 2.10. Concentrations of (a) dissolved SiO_2 , (b) dissolved As(V) and (c) total and dissolved iron concentrations during electrocoagulation of solutions initially containing 100 $\mu\text{g/L}$ As(V) at pH 7.

Possible reasons for the different effects are the differences in the inhibitory mechanisms. In this study, since silica did not have as strong an affinity to the iron oxides as phosphate or arsenic did, it did not significantly inhibit As removal. Although the presence of silica did affect the identity of the iron oxides formed and prevented lepidocrocite formation (Figure 2.3), the other iron oxides that formed (potentially

ferrihydrite) could also serve as sorbents for arsenic removal. However, in the study by Zeng et al. (2008a), silica may have polymerized and physically blocked access to adsorption sites within internal pores of the iron oxide-based sorbent.

2.3.7 Effect of Sulfate on As Removal

The presence of 10 and 50 mg/L SO_4^{2-} (Figure 2.11) did not affect the removal of As.

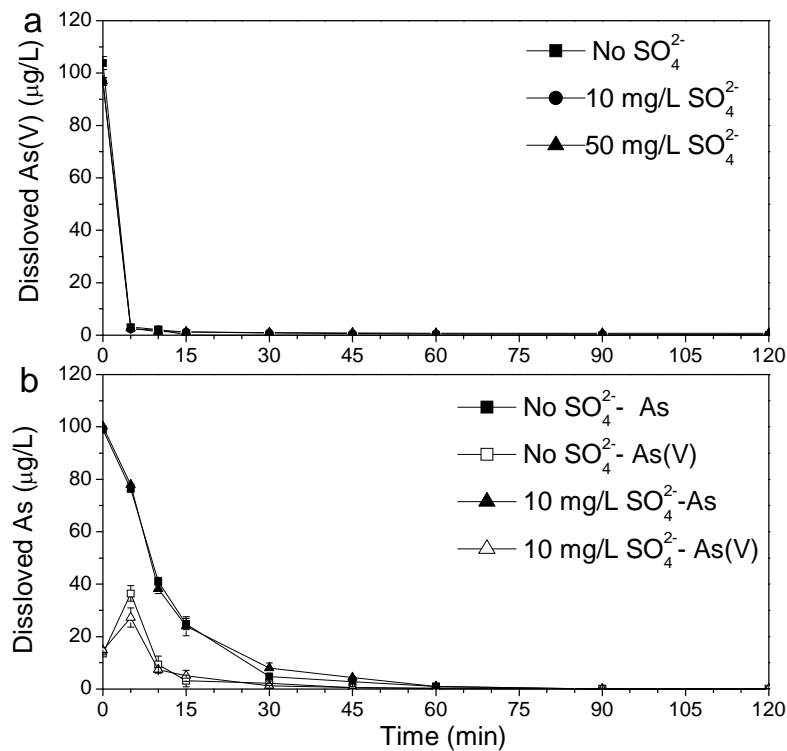


Figure 2.11. Dissolved concentrations of arsenic during electrocoagulation of solutions initially containing (a) 100 µg/L As(V) and (b) 100 µg/L As(III) at pH 7. Panel (b) also shows the concentration of dissolved As(V).

Meng et al. (2000) also reported that the presence of 6.8-204 mg/L SO_4^{2-} had no significant effects on the final removal efficiency of As(III) during equilibrium adsorption experiments. Because sulfate did not affect lepidocrocite formation, and does

not adsorb as strongly as As(V) and phosphate, it is not surprising that sulfate did not affect the performance of the electrocoagulation process.

2.3.8 Results of the Field Study

The treated water from the field units was collected and analyzed in the lab for arsenic, phosphate and iron. Table 2.3 shows the performance of the EC units installed in the field. Barring a few, all the units were able to reduce arsenic to less than 10ppb levels after candle filtration. These units were not being operated properly as per the instructions.

Table 2.3. Arsenic removal by the domestic EC units installed at the field sites

Sl. no.	User's Name	pH	initial (ppb)			settled (ppb)		filtered (ppb)	
			As tot	As (V)	P	As tot	P	As tot	P
1	Pravin Bag	7.1	526	124.5	203	13.3	n.d.	0.4	n.d.
2	Sanjay Bag	7.1	526	124.5	203	9.4	n.d.	0.2	n.d.
3	Arobindo Chakraborty		483.5		198	12.7	n.d.	n.d.	n.d.
4	Kamal Bisas	6.8	448.5	92	182	13.6	n.d.	n.d.	n.d.
5	Kalidas Bag	6.8	448.5	92	182	8.2	n.d.	n.d.	n.d.
6	Prosun Bag		482.5		192	12.1	n.d.	n.d.	n.d.
7	Gauri Sarkar	7	676.5	102.5	253	16.9	n.d.	n.d.	n.d.
8	Madan Barik		526		198	24.1	n.d.	n.d.	n.d.
9	Uttam Bag		675		753	11.8	n.d.	3.9	n.d.
10	Dr. Krishna Pal	7	676.5	102.5	753	11.9	n.d.	0.5	n.d.
11	Nirbhada Mondal		487.5		144	7.9	n.d.	4.5	n.d.
12	Manik Mondal		448.5		156	12.6	3	n.d.	n.d.
13	Bimal Bisas		526.5		193	14.7	3	n.d.	n.d.
14	Promotho Bag		482.5		178	30.7	5	5.8	n.d.
15	Vivek Bisas (Lalmath)	6.2	710	29	781	52.3	12	52.3	12
16	Sanatan Barik		526.5		198	48.5	21	10.3	2
17	Batu Bag		481.5		219	50.4	33	26.4	5
18	Sachin	7	676.5	102.5	753	50.9	31	25.8	4

*n.d. - not detectable

It can be clearly seen from the table 2.3 and Figure 2.12 that the untreated water arsenic concentrations are very high, in the range of 400-700ppb. Most of the samples also have very high phosphate concentrations. In the final filtered water samples the arsenic concentration is seen to reduce to less than 10ppb in most samples and the phosphate concentrations also went to below detectable limits in these. But samples 15, 16, 17 and 18 were seen to have higher arsenic concentration in the filtered water. On further investigation it was found that the users of these units were not following the instructions for use of the domestic EC setup by either not aerating the water (i.e. the aquarium pump was not switched on) or were carrying EC for less time duration (less than the 3hrs. as suggested by us).

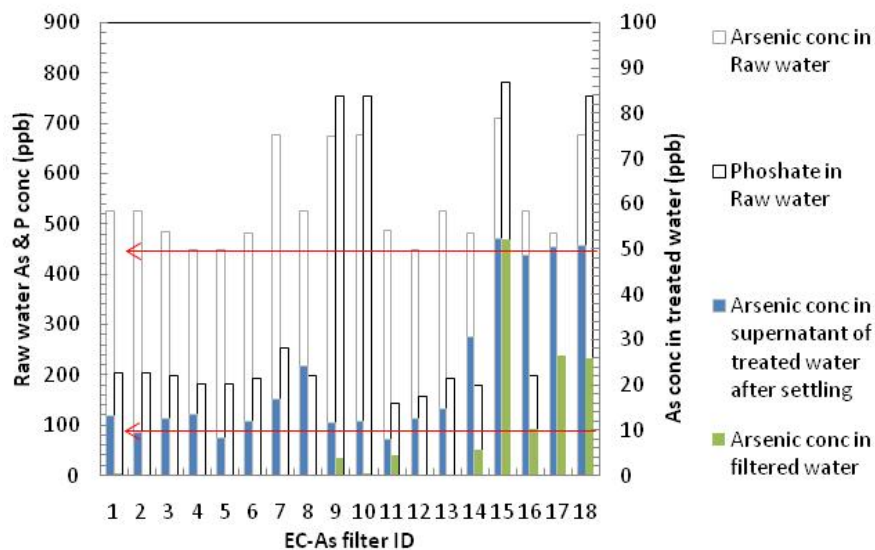


Figure 2.12. Domestic EC setup results from the field study. The red arrows indicate the WHO guideline value for arsenic in drinking water (10ppb) and the Indian standards for arsenic in drinking water (50ppb)

Also to be noted here is the arsenic concentration achieved after just EC followed by settling before the filtration step. There is significant arsenic reduction in the supernatant. But to achieve the drinking water standards the filtration step is found to be essential.

2.4 Conclusions

The iron generated during electrocoagulation was present in solid phases as lepidocrocite. Arsenic removal by electrocoagulation involved lepidocrocite formation followed by arsenic adsorption. As removal was slower at higher pH and higher initial arsenic concentrations. As(III) was partially oxidized to As(V) during electrocoagulation. As(V) removal was faster than As(III) removal. Phosphate inhibited As removal by acting as a competing adsorbate and possibly by delaying the oxidation of Fe(II) to produce lepidocrocite. Although silica prevented the formation of lepidocrocite, arsenic removal was still very rapid and extensive by adsorption to the more amorphous iron oxides that formed. Sulfate had no significant effect on As removal or coagulant formation. Over 99 % arsenic removal efficiency could be achieved in both the laboratory and the field study.

2.5 Acknowledgments

The project was supported by the McDonnell Academy Global Energy and Environment Partnership of Washington University. The field study was performed with the financial support of the Indian Department of Science and Technology. The authors are grateful to Kate Nelson for her analytical assistance.

2.6 References

- Amstaetter, K., Borch, T., Larese-Casanova, P., Kappler, A., 2010. Redox transformation of arsenic by Fe(II)-activated goethite (α -FeOOH). *Environmental Science & Technology*, 44, 102-108.
- Balasubramanian, N., Madhavan, K., 2001. Arsenic removal from industrial effluent through electrocoagulation. *Chemical Engineering and Technology*, 24, 519-521.
- Bisceglia, K.J., Rader, K.J., Carbonaro, R.F., Farley, K.J., Mahony, J.D., Di Toro, D.M., 2005. Iron(II)-catalyzed oxidation of arsenic(III) in a sediment column. *Environmental Science & Technology*, 39, 9217-9222.
- Ciardelli, M.C., Xu, H.F., Sahai, N., 2008. Role of Fe(II), phosphate, silicate, sulfate, and carbonate in arsenic uptake by coprecipitation in synthetic and natural groundwater. *Water Research*, 42, 615-624.
- Davis, C.C., Knocke, W.R., 2001. Edwards M. Implications of aqueous silica sorption to iron hydroxide: Mobilization of iron colloids and interference with sorption of arsenate and humic substances. *Environmental Science & Technology*, 35, 3158-3162.
- Dhar, R. K., Zheng, Y., Rubenstone, J., Van Geen, A., 2004. A rapid colorimetric method for measuring arsenic concentrations in groundwater. *Analytica Chimica Acta*, 526, 203-209.
- Dixit, S., Hering, J. G., 2003. Comparison of arsenic(V) and arsenic(III) sorption onto iron oxide minerals: Implications for arsenic mobility. *Environmental Science & Technology*, 37, 4182-4189.
- Jain, C.K., Ali, I., 2000. Arsenic: occurrence, toxicity and speciation techniques. *Water Research*, 34, 4304-4312.
- Kumar, P.R., Chaudhari, S., Khilar, K.C., Mahajan, S. P., 2004. Removal of arsenic from water by electrocoagulation. *Chemosphere*, 55, 1245-1252.
- Lakshmanan, D., Clifford, D.A., Samanta, G., 2009. Ferrous and ferric ion generation during iron electrocoagulation. *Environmental Science and Technology*, 43, 3853-3859.
- Meng, X.G., Bang, S., Korfiatis, G.P., 2000. Effects of silicate, sulfate, and carbonate on arsenic removal by ferric chloride. *Water Research*, 34, 1255-1261.
- Meng, X.G., Korfiatis, G.P., Bang, S.B., Bang, K.W., 2002. Combined effects of anions on arsenic removal by iron hydroxides. *Toxicology Letters*, 133, 103-111.
- Parga, J.R., Cocke, D.L., Valenzuela, J.L., Gomes, J.A., Kesmez, M., Irwin, G., Moreno, H., Weir, M., 2005. Arsenic removal via electrocoagulation from heavy metal

contaminated groundwater in La Comarca Lagunera Mexico. *Journal of Hazardous Materials*, 124: 247-254.

Peacock, C.L., Sherman, D.M., 2004. Copper(II) sorption onto goethite, hematite and lepidocrocite: A surface complexation model based on ab initio molecular geometries and EXAFS spectroscopy. *Geochimica et Cosmochimica Acta* , 68,2623-2637.

Sahai, N., Lee, Y.J., Xu, H.F., Ciardelli, M., Gaillard, J.F., 2007. Role of Fe(II) and phosphate in arsenic uptake by coprecipitation. *Geochimica et Cosmochimica Acta*, 71 , 3193-3210.

Schwertmann, U., Cornell, R.M., 2000. *Iron oxides in the laboratory: preparation and characterization*. Wiley-VCH, Weinheim.

Stumm, W., Morgan, J.J., 1996. *Aquatic Chemistry, chemical equilibria and rates in natural waters*, 3rd ed. John Wiley & Sons, Inc., New York.

Thella, K., Verma, B., Srivastava, V.C., Srivastava, K.K., 2008. Electrocoagulation study for the removal of arsenic and chromium from aqueous solution. *Journal of Environmental Science and Health . Part A: Environmental Science and Engineering and Toxicology* 43, 554-562.

United States Environmental Protection Agency,2002. Implementation guidance for the arsenic rule--drinking water regulations for arsenic and clarifications to compliance and new source contaminants monitoring. EPA/816/K-02/018. U.S. EPA Office of Water, Washington,DC.

Voegelin, A., Kaegi, R., Frommer, J., Vantelon, D., Hug, S.J., 2010. Effect of phosphate, silicate, and Ca on Fe(III)-precipitates formed in aerated Fe(II)- and As(III)-containing water studied by X-ray absorption spectroscopy. *Geochimica et Cosmochimica Acta* 74,164-186.

World Health Organization,1993. *Guidelines for drinking water quality: Remediations*, vol. 1 (3rd ed.). Geneva: WHO.

Wilkie, J.A., 1997. PhD Dissertation, University of California, Los Angeles, CA.

Zeng, H., Arashiro, M., Giammar, D.E., 2008a. Effects of water chemistry and flow rate on arsenate removal by adsorption to an iron oxide-based sorbent. *Water Research*, 42, 4629-4636.

Zeng, H., Fisher, B., Giammar, D.E.,2008b. Individual and competitive adsorption of arsenate and phosphate to a high-surface-area iron oxide-based sorbent. *Environmental Science and Technology*, 42, 147-152.

Chapter 3

Lepidocrocite Generation and Arsenate Removal during Electrocoagulation

This chapter is being as a manuscript for submission to *Environmental Science & Technology*

Abstract

Electrocoagulation is a water treatment technology that involves electrolytic oxidation of anode materials to produce a coagulant *in situ*. Electrocoagulation experiments for arsenic removal were performed using iron electrodes at pH 5, 7 and 9. The effect of water chemistry and treatment time were interpreted using adsorption modeling and a rate model for coagulant production and arsenic adsorption. The iron generated during electrocoagulation was released as Fe(II) and then oxidized to Fe(III) and precipitated as lepidocrocite (γ -FeOOH). Arsenic removal by electrocoagulation involved arsenic adsorption to lepidocrocite. Equilibrium As(V) adsorption was investigated in batch experiments as a function of dissolved As(V) concentration, pH, and phosphate using lepidocrocite generated by electrocoagulation. A surface complexation model was then developed that successfully simulated equilibrium As(V) adsorption. As(V) adsorption generally decreased with increasing pH from 4 to 10. The presence of 1-4 mg P/L of phosphate inhibited As(V) adsorption, and the competitive adsorption was interpreted using a surface complexation model. The rate model simulated overall arsenic removal well by using Faraday's law to predict coagulant production and a rate expression for As adsorption. A maximum arsenic removal efficiency of over 99 % was achieved during both electrocoagulation and equilibrium adsorption experiments.

3.1 Introduction

Arsenic occurs in groundwater through both natural and anthropogenic process (1).

Arsenic is toxic and exposure to arsenic through drinking water is a great threat to human health (1). Considering the high toxicity of arsenic, the World Health Organization (WHO) and USEPA set a maximum acceptable level of arsenic in drinking water to be 10 µg/L (2-3). Arsenic contamination of groundwater is found in both developed and developing countries (4-7). Methods for arsenic removal are widely needed.

Electrocoagulation involves electrolytic oxidation of a metal anode to generate metal oxide and oxyhydroxide coagulants *in situ* (8-10). Electrocoagulation is an alternative to using chemical coagulants for arsenic removal and thus is beneficial for communities with better access to electricity than to chemicals. When iron electrodes are used and sufficient dissolved oxygen is present, an iron oxyhydroxide precipitate forms (11). Previous studies have demonstrated arsenic removal from water and wastewater by electrocoagulation and found that removal involved metal oxide formation followed by arsenic adsorption to the metal oxide (8-10).

The pH of the water influences arsenic removal by electrocoagulation by affecting arsenic species distribution, the surface charge of the metal oxides, and the rate of Fe(III) production from the Fe(II) released from the iron anode (8,11). As(V) adsorption decreases with increasing pH and Fe(II) oxidation is faster at high pH (11-12).

Iron oxides have been widely used as sorbents for arsenic removal because they have strong affinities for arsenic and can have large specific surface areas (4-7). Surface complexation models (SCM) have successfully described the pH-dependence of As(V)

adsorption (4-7, 12). The competition of As(V) and phosphate adsorption onto iron oxide-based sorbents was also simulated successfully by surface complexation models (7,12).

The objectives of this study were to: (1) investigate the effects of dissolved As(V) concentration, pH and phosphate on As(V) adsorption to the iron oxides generated by electrocoagulation, (2) develop a surface complexation model to simulate equilibrium As(V) adsorption, and (3) prepare an overall model for the performance of an electrocoagulation system for As(V) removal.

3.2 Materials and Methods

3.2.1 Electrocoagulation Experiments

The electrocoagulation reactor consisted of a 1 L glass beaker with two iron rods immersed in the aqueous solution. The rods had diameters of 1.75 cm, lengths of 20 cm, and were placed 2 cm apart in the arsenic containing solution. The total submerged surface area of each electrode was 57 cm². Before each experiment, the electrodes were abraded with sand paper to remove scales and then cleaned with 1 M HNO₃ and ultrapure water. A direct current was applied at 12 V to the terminal electrodes from a direct current power supply. The electric current was monitored over the course of each two hour experiment. To provide enough oxygen for the formation of Fe(III) precipitates, the solution was sparged with air at a flow rate of 60 mL/min. The arsenic-containing solution was magnetically-stirred (200 rpm). Duplicate runs were carried out for each experimental condition.

All solutions were prepared with ultrapure water. To prepare each solution, desired volumes of stock solutions were added to the 1 L glass beaker. An As(V) stock solution was made from $\text{Na}_2\text{HAsO}_4 \cdot 7\text{H}_2\text{O}$, and a phosphate stock solution was made from $\text{Na}_2\text{HPO}_4 \cdot 7\text{H}_2\text{O}$. In order to provide pH buffering, NaHCO_3 was added to achieve a concentration of 1 mM. The pH of the As-containing solution in each beaker was periodically readjusted to the target value by adding aliquots of 1 M HNO_3 or 1 M NaOH .

The pH of the solution in the beaker was measured with a pH electrode when the current was not applied. It took about 1 min to adjust the pH to the desired values. Considering the time used to adjust pH, each experiment lasted about 130 min, although current was only applied during 120 minutes of the experiment.

3.2.2 Equilibrium Adsorption Experiments

Equilibrium adsorption of As(V) to the solids generated during electrocoagulation was investigated in batch experiments as a function of dissolved As(V) concentration, pH, and phosphate concentration. Since As(V) adsorption may be far from equilibrium during electrocoagulation, the iron oxides for batch experiments were first generated by electrocoagulation in the absence of arsenic and then they were equilibrated with arsenic in batch suspensions. The electrocoagulation reactor was operated without As at pH 7 for 2 hours to generate enough iron oxide for adsorption experiments. The iron oxide suspension was allowed to settle overnight, the supernatant was decanted, and the resulting concentrated suspension was used as the sorbent stock suspension for the equilibrium adsorption experiments. The concentration of this stock suspension was

determined to be 0.4 g/L by measuring its total iron concentration and assuming that all of the iron was present as lepidocrocite. The solid phase collected from a parallel experiment was freeze-dried for characterization.

Experiments to develop data for an adsorption isotherm at pH 4 used 10 mL concentrated iron oxide suspension, aliquots of As(V) stock solution to provide a wide range of total As(V) concentration, and sufficient ultrapure water to have 50 mL suspensions. The lepidocrocite solid concentration in the suspensions was 0.079 g/L, and the ionic strength was fixed by addition of NaHCO₃ to 1 mM. The pH dependence of As(V) adsorption was determined in similar experiments with a fixed 100 µg/L (1.3 µM) or 1000 µg/L (13.3 µM) As(V) concentration over a pH range from 4 to 10. These experiments to study the pH-dependence of adsorption were performed in the absence and in the presence of 1 mg P/L (32.2 µM) or 4 mg P/L (129 µM) of phosphate. Separate experiments were conducted to determine phosphate adsorption as a function of pH at 1 mg P/L of phosphate both with and without 100 µg/L (13.3 µM) As(V). The pH of the series of suspensions was adjusted to the desired value in the range of 4-10 by addition of 1 M NaOH and 1 M HNO₃. All batch reactors were equilibrated for 24 h with mixing provided by a platform shaker (New Brunswick Scientific, NJ) at 50 rpm.

3.2.3 Sampling Methods

For the electrocoagulation experiments using As(V), 15 mL samples of solution were periodically collected from the beaker. For the equilibrium adsorption experiments using As(V) and phosphate, 15 mL was collected from each batch reactor after the 24 h equilibration period. For both the electrocoagulation and adsorption experiments, 7.5 mL

of each 15 mL sample were filtered using 0.45 μm filter membranes (polyethersulfone, Fisher Scientific), and the filtrate were acidified to 1% HNO_3 . The remaining 7.5 mL of unfiltered suspension was acidified to 1% HNO_3 by addition of concentrated HNO_3 , which completely dissolved the suspended solids.

3.2.4 Analysis Methods

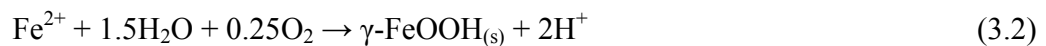
The filtered and acid-treated samples were analyzed for dissolved and total concentrations of constituents, respectively. The concentrations of As, Fe and P were determined by inductively coupled plasma mass spectrometry (ICP-MS) (7500ce, Agilent Technologies, Santa Clara, CA). The instrument detection limits for As, Fe, and P were 0.1 $\mu\text{g/L}$, 0.05 mg/L and 0.01 mg/L , respectively. Selected filtered samples were analyzed for Fe(II) using the ferrozine method. The specific surface areas (SSA) of the freeze-dried solids were measured by the BET (Brunauer-Emmett-Teller) N_2 -adsorption method (Autosorb-1-C, Quantachrome, U.S.A.). X-ray powder diffraction (XRD) patterns were collected using $\text{Cu K}\alpha$ radiation (D-MAX/A, Rigaku, Japan). The size and morphology of the iron oxide particles were determined using transmission electron microscopy (TEM) (JEOL 2100F, Japan). Dissolved oxygen for selected samples was measured using a Hach Surface Water Test Kit (Fondriest Environmental, Inc.).

3.3 Results and Discussion

3.3.1 Production of Iron Oxide Coagulants by Electrocoagulation

During the experiment, the solution changed from colorless to reddish brown. The total iron concentrations increased linearly with reaction time (Figure 3.1b). In this study, the

reported values are the average plus the standard deviation. For all the electrocoagulation experiments, about 50 mg/L (average value was 50.5 mg/L) of total iron was produced in 2 hours. The reactor was operated with a current of 22 mA, and the total iron produced was consistent with a value of 52.2 mg/L predicted by Faraday's Law for the oxidation of the iron electrode to dissolved Fe(II). Fe is released to solution as Fe(II) and is then oxidized to Fe(III) by the dissolved oxygen (11). The Fe(III) precipitated to form iron oxides or oxyhydroxides (Reactions 3.1 and 3.2). At the cathode hydrogen gas is generated.



During one set of experiments, the dissolved oxygen (DO) was measured and the value was near 10 mg/L for all samples collected (30, 60 and 90 min), which indicated that the solution was saturated with dissolved oxygen. The dissolved iron concentrations were very low when compared with the total iron concentrations in each experiment, which indicated that nearly all of the iron was present in the solid phases.

The solids were identified as lepidocrocite ($\gamma\text{-FeOOH}$) by their XRD patterns both in the presence and absence of phosphate (Figure A1 in the Appendix). The lepidocrocite particles were 100-200 nm long and about 5-20 nm wide (Figure A2 in the Appendix). The specific surface area of the solids was 200.5 m²/g and was independent of the solution composition. It is well documented that lepidocrocite can be synthesized by oxidizing Fe(II) solutions using dissolved oxygen at ambient temperature (13). The rate of Fe(II) oxidation is known to increase with increasing pH (11,14).

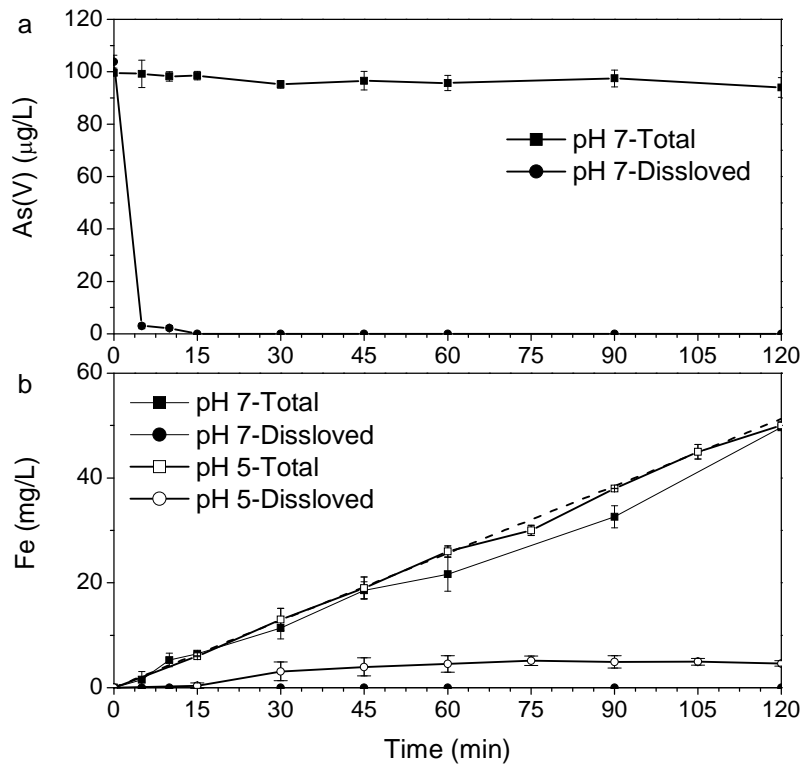


Figure 3.1. Concentrations of total and dissolved (a) As(V) at pH 7.0 and (b) iron during electrocoagulation of a solution initially containing 100 µg/L As(V) at pH 5.0 and 7.0. The dashed line in (b) represents the total iron concentration predicted by the Faraday's law at the measured current of 22 mA.

Although experiments results did find measurable dissolved iron at pH 5 that was not present at pH 7 or 9, the dissolved Fe was not determined to be Fe(II). The measured dissolved iron concentrations measured at pH 5 were higher than the equilibrium solubility of lepidocrocite, so the dissolved iron may represent colloidal Fe(III) species or Fe(II) that, for unknown reasons, was not measurable by the ferrozine method.

3.3.2 As(V) Equilibrium Adsorption in the Absence of Phosphate

The As(V) adsorption density at pH 4 increased with increasing dissolved As(V) concentration until the surface sites of the lepidocrocite were saturated (Figure 3.2). By fitting the adsorption data to the Langmuir isotherm (Equation 3.3), the maximum adsorption density was obtained as 19.8 $\mu\text{g As(V) /mg FeOOH}$ and K_L was found to be 0.006 L/ μg .

$$\Gamma = \frac{\Gamma_{\max} K_L C}{1 + K_L C} \quad (3.3)$$

In equation 3, Γ is the amount of As(V) adsorbed by per unit of lepidocrocite ($\mu\text{g As(V) /mg FeOOH}$), Γ_{\max} is the maximum amount of As(V) adsorbed by per unit of lepidocrocite ($\mu\text{g As(V) /mg FeOOH}$), K_L is the adsorption constant (L/ μg), and C is the dissolved As(V) concentration at equilibrium ($\mu\text{g/L}$).

As(V) adsorption onto the lepidocrocite decreased with increasing pH from 4 to 10 at total As(V) concentrations of 100 and 1000 $\mu\text{g/L}$ (Figure 3.3). A surface complexation model with the diffuse double layer to account for electrostatic contributions to adsorption was used to describe the As(V) adsorption edges in this study (4). Reactions and parameters used in the surface complexation model are listed in Table 1. The constants for surface protonation of lepidocrocite were taken from the study by Peacock and Sherman (16). They modeled Cu(II) adsorption using bidentate and tridentate surface complexes with lepidocrocite and a surface site density of 1.6 sites/ nm^2 . The surface site concentration was determined from Γ_{\max} in the adsorption isotherm to be 2.09×10^{-5} M. When considering the specific surface area of the lepidocrocite and

assuming that each adsorbed As(V) occupies a single surface site, the maximum adsorption density corresponds to a surface site density of 0.8 sites/nm^2 . This site is lower than those reported by Dixit and Hering (2.6 sites/nm^2) (4) and Zeng et al. (1.5 sites/nm^2) (12). The difference in the site concentrations between this study and these previous studies may result from the different kinds of iron oxides used (lepidocrocite versus goethite and amorphous iron oxides). If adsorption occurs through bidentate coordination to two surface sites, then the site density in this study would be 1.6 sites/nm^2 .

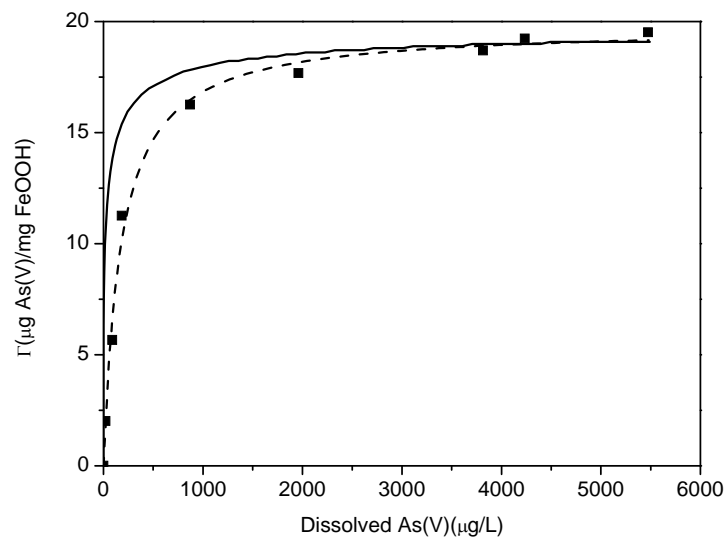


Figure 3.2. As(V) adsorption isotherm onto lepidocrocite at pH 4. Data are shown as symbols and simulations are shown as lines. The solid line is the surface complexation model and the dashed line is the Langmuir isotherm.

The surface complexation constants for As(V) adsorption were systematically varied using the computer program MINEQL+ 4.6 (16) to obtain the constants that

provide the best fit of the model to the experimental data. The equilibrium constants reported by Dixit and Hering for the formation of As(V) surface complexes on hydrous ferric oxide were used as the starting points (4). The optimized constants are listed in Table 3.1.

Table 3.1. Reactions and parameters used for surface complexation modeling of As(V) and phosphate to the lepidocrocite generated from electrocoagulation.

Reaction	LogK	Reference
surface protonation		
$\equiv\text{FeOH} + \text{H}^+ = \equiv\text{FeOH}_2^+$	6.69	(15)
$\equiv\text{FeOH} = \equiv\text{FeO}^- + \text{H}^+$	-8.69	
arsenate adsorption		
$\equiv\text{FeOH} + \text{AsO}_4^{3-} + 3\text{H}^+ = \equiv\text{FeH}_2\text{AsO}_4 + \text{H}_2\text{O}$	30.28*	This study
$\equiv\text{FeOH} + \text{AsO}_4^{3-} + 2\text{H}^+ = \equiv\text{FeHAsO}_4^- + \text{H}_2\text{O}$	22.15*	
$\equiv\text{FeOH} + \text{AsO}_4^{3-} + \text{H}^+ = \equiv\text{FeAsO}_4^{2-} + \text{H}_2\text{O}$	19.38*	
phosphate adsorption		
$\equiv\text{FeOH} + \text{PO}_4^{3-} + 3\text{H}^+ = \equiv\text{FeH}_2\text{PO}_4 + \text{H}_2\text{O}$	30.80	This study
$\equiv\text{FeOH} + \text{PO}_4^{3-} + 2\text{H}^+ = \equiv\text{FeHPO}_4^- + \text{H}_2\text{O}$	21.15	
$\equiv\text{FeOH} + \text{PO}_4^{3-} + \text{H}^+ = \equiv\text{FePO}_4^{2-} + \text{H}_2\text{O}$	19.80	
arsenate protonation		
$\text{AsO}_4^{3-} + \text{H}^+ = \text{HAsO}_4^{2-}$	11.50	(16)
$\text{AsO}_4^{3-} + 2\text{H}^+ = \text{H}_2\text{AsO}_4^-$	18.46	
$\text{AsO}_4^{3-} + 3\text{H}^+ = \text{H}_3\text{AsO}_4$	20.70	
phosphate protonation		
$\text{PO}_4^{3-} + \text{H}^+ = \text{HPO}_4^{2-}$	12.375	(16)
$\text{PO}_4^{3-} + 2\text{H}^+ = \text{H}_2\text{PO}_4^-$	19.573	
$\text{PO}_4^{3-} + 3\text{H}^+ = \text{H}_3\text{PO}_4$	21.721	

*The constants used by Dixit and Hering (4) are 29.88, 24.43 and 18.10, respectively.

The As(V) adsorption edge on the iron oxides could be described very well for both 100 and 1000 $\mu\text{g/L}$ total As(V) using the surface complexation model (Figure 3.3). In addition, the intrinsic As(V) surface complexation constants obtained in this study were very similar to those obtained by Dixit and Hering (4). The intrinsic As(V) surface complexation constants obtained in this study could also provide a satisfactory simulation of the As(V) adsorption isotherm at pH 4 (Figure 3.2).

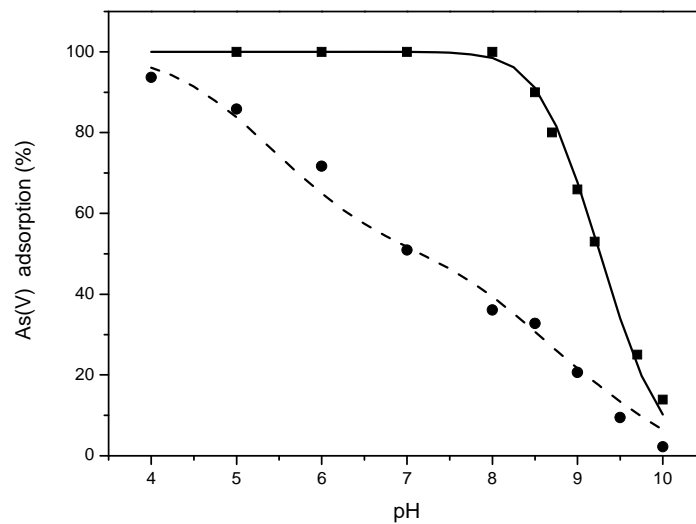


Figure 3.3. As(V) adsorption edges onto lepidocrocite at initial As(V) concentrations of 100 (■) and 1000 $\mu\text{g/L}$ (●). Data are shown as symbols and simulations from the surface complexation model as lines.

3.3.3 As(V) Equilibrium Adsorption in the Presence of Phosphate

The presence of 1-4 mg P/L of phosphate inhibited As(V) adsorption onto the lepidocrocite (Figure 3.4). Phosphate can compete with As(V) for the surface sites. To obtain constants for phosphate surface complexation reactions, phosphate (1 mg P/L)

adsorption was investigated from pH 4-10 in the absence of As(V) and then simulated using the surface complexation model (Figure 3.5 and Table 3.1). The surface complexation constants for phosphate adsorption were systematically varied using the computer program MINEQL+ 4.6 to obtain the optimal constants for fitting the model to the adsorption data. The values for As(V) adsorption equilibrium constants were used as the starting points. The optimized constants are listed in Table 3.1. The phosphate (1 mg P/L) adsorption edge in the absence of As(V) could be described well using the surface complexation model (Figure 3.5).

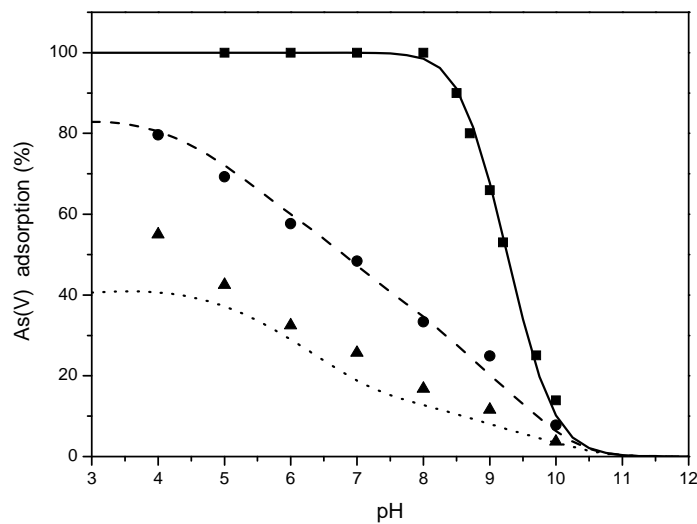


Figure 3.4. As(V) adsorption edges onto lepidocrocite for 100 µg/L total As(V) in the absence of phosphate (■) and in the presence of 1 (●) and 4 (▲) mg P/L of phosphate. Data are shown as symbols and simulations from the surface complexation model are shown as lines.

The reactions and constants in Table 3.1 were then used to simulate the concurrent adsorption of As(V) and phosphate onto lepidocrocite (Figures 3.4-5).

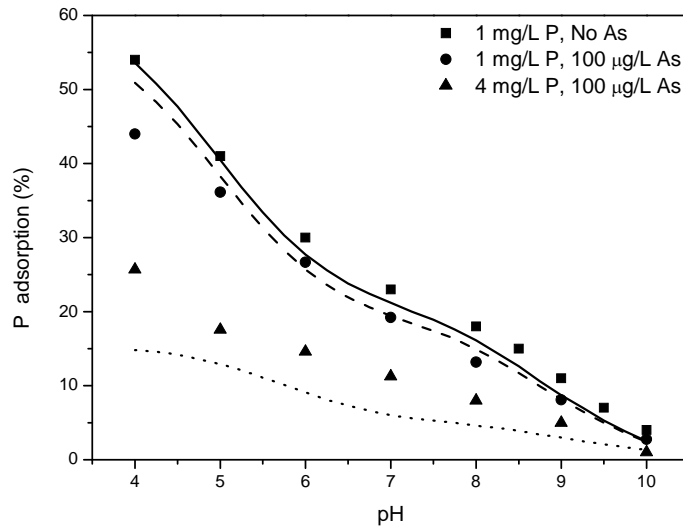


Figure 3.5. Phosphate adsorption edges onto lepidocrocite in the absence of As(V) and in the presence of 100 µg/L As(V). Data are shown as symbols and simulations from the surface complexation model are shown as lines.

The surface complexation model simulated As(V) adsorption to lepidocrocite in the presence of 1 mg P/L very well, but the model underestimated As(V) adsorption onto lepidocrocite in the presence of 4 mg P/L. This underestimation of As(V) adsorption may be caused by an overestimation of phosphate adsorption. It should be noted that phosphate adsorption was predicted using a model optimized for 1 mg P/L and did not use any data for As-free conditions with 4 mg P/L. The model may overestimate phosphate adsorption at the higher phosphate loading, which could happen if the surface

sites were actually distributed between strong and weak sites, which would then overestimate the inhibition of arsenate caused by the phosphate.

3.3.4 Overall Reactor Model for As(V) Removal by Electrocoagulation

In the electrocoagulation process, the rate of As(V) removal can be assumed to be proportional to the difference between the actual and the equilibrium dissolved concentration of As(V) (i.e. the driving force) and the amount of solid lepidocrocite present (Equation 3.4).

$$-\frac{dC}{dt} = k(C - C_{eq})C_{lep} \quad (\text{Initial condition: } C = C_o \text{ at } t=0) \quad (3.4)$$

The dissolved As(V) concentration (C in $\mu\text{g/L}$) and the solid lepidocrocite concentration (C_{lep} in $\mu\text{g/L}$) are changing with time. Because the predicted equilibrium concentration C_{eq} is determined by the dissolved As(V) and the amount of solid, it too will change with time. However for this study the final dissolved As(V) concentration in the reactor after two hours of treatment was used to represent C_{eq} . C_o is the initial dissolved As(V) concentration in the reactor and k is the reaction constant ($\text{L}/(\mu\text{g}\cdot\text{min})$).

Faraday's Law (equation 3.5) was used to predict iron formation.

$$m = \frac{MI}{Fz} t * 60 \quad (3.5)$$

In equation 3.5, m is the mass of the iron produced at the anode (g), M is the atomic weight of iron (56 g/mol), I is the current applied to an electrode ($I=0.022$ A), F is the Faraday constant (96485 C/mol), z is the valence number of the iron ($z=2$), t (min) is the total time the current was applied, and 60 is the conversion factor between minutes and

seconds. Assuming that all iron is released as Fe(II) and precipitates as the oxyhydroxide lepidocrocite, the lepidocrocite generation rate can be expressed as equation 3.6.

$$C_{lep} = k_{lep}t \quad (3.6)$$

In equation 6, k_{lep} ($\mu\text{g}/(\text{L}\cdot\text{min})$) is the lepidocrocite generation constant. In this study k_{lep} is calculated to be $609 \mu\text{g}/(\text{L}\cdot\text{min})$, thus $C_{lep} = 609t$. Although not all iron was present in the solid phase, especially at pH 5 (Figure 3.1b), and at lower pH the assumption of instantaneous oxidation is less valid, the model still worked well.

Substituting $C_{lep} = 609t$ into equation 3.4 and integrating yields equation 3.7.

$$C = C_{eq} + (C_0 - C_{eq})\exp(-304.5kt^2) \quad (3.7)$$

Equation 3.7 was used to simulate As(V) removal by electrocoagulation at pH 5, 7 and 9. The optimal value of k for each pH was determined as the one providing the best fit to the data. The results illustrated that the proposed kinetic model could simulate the As(V) removal by electrocoagulation very well (Figure 3.6 and Table 3.2). The As(V) removal rate was slower at higher pH during electrocoagulation. A similar pH effect was observed by Thella et al., who found that arsenic removal rate decreased with increasing pH from 2 to 8 (17). There were no significant differences among the k values optimized for pH 5 and 7, but they were significantly larger than the value obtained at pH 9 (Table 3.2). At higher pH, the driving force ($C - C_{eq}$) was smaller, but even after accounting for this driving force using equation 4, the rate constant was still lower at pH 9 than at pH 5 and 7. The results demonstrated that both the driving force and the rate constant for adsorption are lower at higher pH.

Table 3.2. Parameters used for simulation of the overall electrocoagulation process for treatment of solutions initially containing 100 µg/L As(V).

pH	k (L/(µg·min))	C _{eq} (µg/L)
5	$5.0 \cdot 10^{-4}$	0
7	$4.6 \cdot 10^{-4}$	0
9	$3.7 \cdot 10^{-6}$	4.1

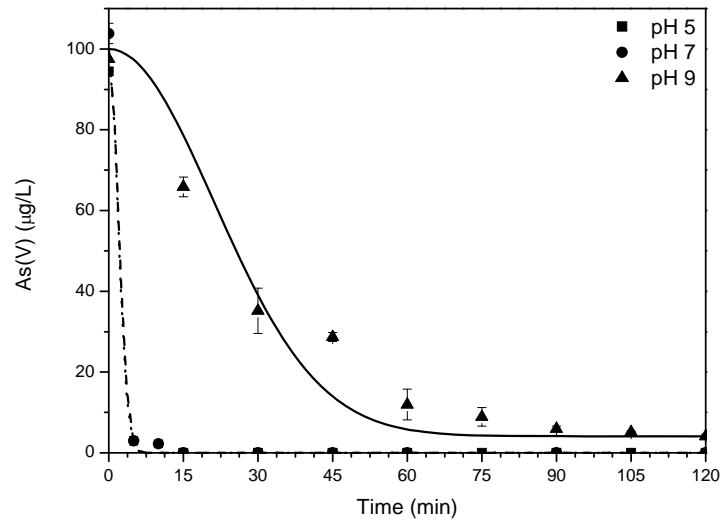


Figure 3.6. Electrocoagulation of solutions initially containing 100 µg/L As(V) at pH 5, 7 and 9. Data are shown as symbols and simulations are shown as lines. Data and simulations at pH 5 are partially obscured by those at pH 7.

The equilibrium dissolved As(V) concentrations predicted using the surface complexation model at the end of the experiments at pH 5 and 7 agreed well with the value of C_{eq} from the simulation using the rate model. However, the equilibrium dissolved As(V) concentration predicted using the surface complexation model at pH 9 (32.3 µg/L) was larger than the value measured at the end of an electrocoagulation

experiment (4.1 $\mu\text{g/L}$) that used in the rate model. One possible reason for this difference is that the lepidocrocite particles grow with the reaction time; thus, the particles during electrocoagulation (age ≤ 2 hours) may be smaller than those (age > 2 hours) used for As(V) adsorption experiments. The lepidocrocite during electrocoagulation would then have a larger specific surface area than during As(V) adsorption experiments, and consequently, more adsorption could occur during electrocoagulation than during batch adsorption.

Another method was also tried for simulating As(V) removal by electrocoagulation. In this method, the equilibrium dissolved As(V) concentration predicted using the surface complexation model at each time t was used for the value of C_{eq} in equation 4. Numerical solutions of this differential equation did not provide better fits of the experimental data at pH 5 and 7 than the approach with a fixed C_{eq} value, and at pH 9 the fits were considerably worse because of the disparity between the value of C_{eq} measured in electrocoagulation experiments and predicted by the surface complexation model.

3.4 Environmental Implications

Electrocoagulation using iron electrodes can produce iron oxyhydroxides *in situ* as a sorbent for As(V) removal. This technology can potentially be used to remove other heavy metals from contaminated drinking water.

As(V) adsorption onto the iron oxyhydroxide generated by electrocoagulation and competitive adsorption of As(V) and phosphate over a wide pH range were predicted successfully by a surface complexation model. The model can be used to predict As(V)

adsorption onto an iron oxyhydroxide based on the water chemistry over a wide range of conditions. Application of the surface complexation modeling approach can be used to assess potential performance of electrocoagulation for arsenic removal for various waters without needing to conduct lengthy experiments.

As(V) removal by electrocoagulation was simulated successfully using a rate model involving simultaneous coagulant production and arsenic adsorption. Such a model can be used as a design tool for predicting As(V) removal by electrocoagulation for different reactor systems.

3.5 Acknowledgments

This project was supported by the McDonnell Academy Global Energy and Environment Partnership of Washington University. The authors thank Sanjeev Chaudhari for his helpful suggestions and Kate Nelson for her analytical assistance.

3.6 Literature Cited

- (1) Jain, C.K.; Ali, I. Arsenic: occurrence, toxicity and speciation techniques. *Water Res.* 2000,34, 4304-4312.
- (2) World Health Organization. *Guidelines for drinking water quality: Remediations*, vol. 1 (3rd ed.); WHO: Geneva, 1993.
- (3) U.S. EPA. *Implementation guidance for the arsenic rule--drinking water regulations for arsenic and clarifications to compliance and new source contaminants monitoring* EPA/816/K-02/018.; U.S. EPA Office of Water: Washington DC, 2002.
- (4) Dixit, S.; Hering, J.G. Comparison of arsenic(V) and arsenic(III) sorption onto iron oxide minerals: Implications for arsenic mobility. *Environ. Sci. Technol.* 2003, 37, 4182-4189.

- (5) Wilkie, J.A.; Hering, J.G. Adsorption of arsenic onto hydrous ferric oxide: Effects of adsorbate/adsorbent ratios and co-occurring solutes. *Colloids and Surfaces A- Physicochemical and Engineering Aspects* 1996,107, 97-110
- (6) Mamindy-Pajany, Y.; Hurel, C.; Marmier, N.; Romeo, M. Arsenic adsorption onto hematite and goethite. *Comptes Rendus Chimie* 2009, 12, 876-881.
- (7) Holm, T.R. Effects of CO_3^{2-} /bicarbonate, Si, and PO_4^{3-} on arsenic sorption to HFO. *Journal American Water Works Association* 2002, 94, 174-181.
- (8) Kumar, P.R.; Chaudhari, S.; Khilar, K.C.; Mahajan, S.P. Removal of arsenic from water by electrocoagulation. *Chemosphere* 2004, 55,1245-1252.
- (9) Balasubramanian, N.; Madhavan, K. Arsenic removal from industrial effluent through electrocoagulation. *Chem. Eng. Tech.* 2001, 24, 519-521.
- (10) Balasubramanian, N.; Kojima, T.; Basha, C.A.; Srinivasakannan, C. Removal of arsenic from aqueous solution using electrocoagulation. *J. Hazard. Mater.* 2009,167: 966-969.
- (11) Lakshmanan, D.; Clifford, D.A.; Samanta, G. Ferrous and ferric ion generation during iron electrocoagulation. *Environ. Sci. Technol.* 2009,43, 3853-3859.
- (12) Zeng, H.; Fisher, B.; Giammar, D.E. Individual and competitive adsorption of arsenate and phosphate to a high-surface-area iron oxide-based sorbent. *Environ. Sci. Technol.* 2008, 42, 147-152.
- (13) Schwertmann, U.; Cornell, R.M. *Iron oxides in the laboratory: preparation and characterization*; Wiley-VCH: Weinheim,2000.
- (14) Stumm, W.; Morgan, J.J. *Aquatic Chemistry, chemical equilibria and rates in natural waters*, 3rd ed; John Wiley & Sons, Inc.: New York, 1996.
- (15) Peacock, C.L.; Sherman, D.M. Copper(II) sorption onto goethite, hematite and lepidocrocite: A surface complexation model based on ab initio molecular geometries and EXAFS spectroscopy. *Geochim. Cosmochim. Acta* 2004, 68,2623-2637.
- (16) Schecher, W. *Thermochemical data used in MINEQL+ version 4.5*; Hallowell: ME, 2001.
- (17) Thella, K.; Verma, B.; Srivastava, V.C.; Srivastava, K.K. Electrocoagulation study for the removal of arsenic and chromium from aqueous solution. *J. Environ. Sci. Health* 2008,43,554-562.

3.7 Appendix

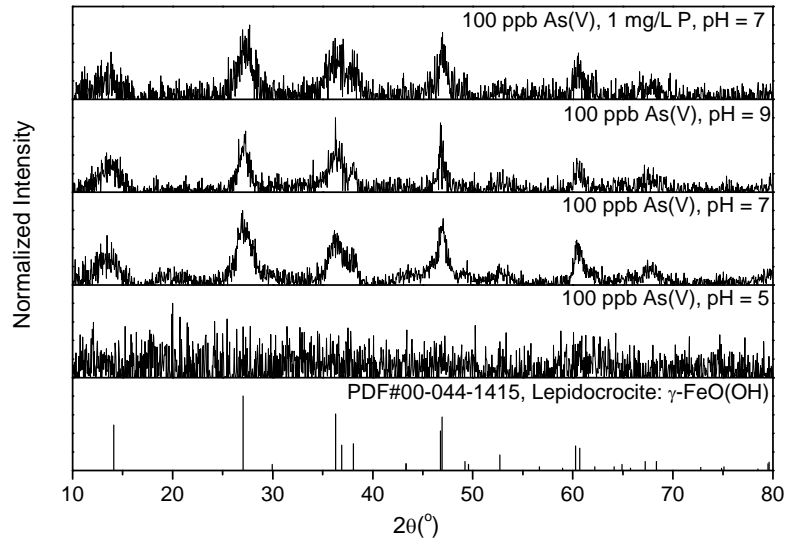


Figure A1. X-ray diffraction patterns of solids generated during experiment. The reference pattern for lepidocrocite is included for comparison.

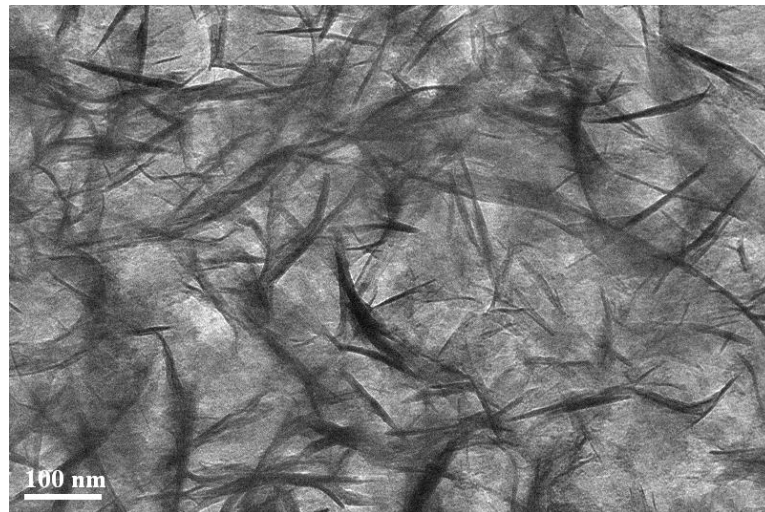


Figure A2. TEM image of solids generated during electrocoagulation.

Chapter 4

Conclusions and Recommendations for Future Work

4.1 Conclusions

The iron generated during electrocoagulation precipitated as lepidocrocite (γ -FeOOH), except when dissolved silica was present. Arsenic was removed by adsorption to the lepidocrocite. Arsenic removal was slower at higher pH. When solutions initially contained As(III), a portion of the As(III) was oxidized to As(V) during electrocoagulation. As(V) removal was faster than As(III) removal. The presence of 1 and 4 mg P/L of phosphate inhibited arsenic removal, while the presence of 5 and 20 mg SiO₂/L of silica or 10 and 50 mg SO₄²⁻/L of sulfate had no significant effect on arsenic removal. For most conditions examined in this study, over 99% arsenic removal efficiency was achieved.

Electrocoagulation experiments for arsenic removal were performed using iron electrodes at pH 5, 7 and 9. The effect of water chemistry and treatment time were interpreted using adsorption modeling and a rate model for coagulant production and arsenic adsorption. Equilibrium As(V) adsorption was investigated in batch experiments as a function of dissolved As(V) concentration, pH, and phosphate using lepidocrocite generated by electrocoagulation. A surface complexation model was then developed that successfully simulated equilibrium As(V) adsorption. As(V) adsorption onto the lepidocrocite generally decreased with increasing pH from 4 to 10. The presence of 1-4 mg P/L of phosphate inhibited As(V) adsorption. The rate model simulated the overall

arsenic removal by electrocoagulation well by using Faraday's law to predict coagulant production and a rate expression for As adsorption. A maximum arsenic removal efficiency of over 99 % was achieved during both the electrocoagulation and equilibrium adsorption experiments.

4.2 Recommendations for Future Work

According to the Faraday's Law, the amount of metal ion generated from the anode during electrocoagulation is proportional to the current applied to the anode, thus the current can affect the amount of metal oxides formed and can affect arsenic removal efficiency and rate during electrocoagulation accordingly. Therefore studies on the effect of current on arsenic removal by electrocoagulation are recommended.

So far, most of the studies on arsenic removal by electrocoagulation were conducted in batch mode due to its simple operation and control. However, large-scale arsenic removal by electrocoagulation would require continuous processes for practical engineering reasons. Thus, more studies on continuous arsenic removal by electrocoagulation are recommended.

There is no agreement on how As(III) is oxidized to As(V) during electrocoagulation. As(III) oxidation to As(V) has previously been proposed to occur with dissolved oxygen as the oxidant and intermediate iron-containing species as rate-enhancing species. As(III) oxidation can also occur when Fe(II) is present with Fe(III) oxyhydroxides, and the mechanism has been proposed to involve the formation of an Fe(IV) intermediate. During electrocoagulation, As(III) can be oxidized to As(V) by the

electrodes. Thus, more studies on how As(III) is oxidized to As(V) during electrocoagulation are recommended.

Because there are limited studies of adsorption of As(V) and other solutes to lepidocrocite, additional research can help identify adsorption mechanisms and refine surface complexation models. Direct characterization of arsenic adsorbed onto lepidocrocite using Fourier transform infrared spectroscopy (FTIR) and extended X-ray absorption fine structure (EXAFS) spectroscopy are recommended to determine the molecular-scale structure of adsorbed arsenic. Additional adsorption and potentiometric titration experiments with lepidocrocite could generate data to further constrain the surface site density used in surface complexation modeling.

Finally, after arsenic removal by electrocoagulation, the dissolved arsenic is adsorbed to the iron oxides. If handled improperly, these iron oxides with adsorbed arsenic can cause secondary contamination. Thus more studies are recommended on the disposal of the arsenic-rich iron oxide residual solids from electrocoagulation treatment.

Vita

Wei Wan

Date of Birth July 24, 1984

Place of Birth China

Degrees M.E. Environmental Science and Engineering
Tsinghua University, China, July 2008

B.E. Environmental Engineering
Beijing Technology and Business University, China, July 2006

May 2010

Arsenic Removal Electrocoagulation, Wan, M.S. 2010